„BABEŞ –BOLYAI" UNIVERSITY
FACULTY OF PHYSICS

SIMONA LUPŞOR

LOCAL STATES AND MAGNETIC INTERACTIONS STUDY OF TRANSITION METAL IONS IN VITREOUS OXIDE MATRICES

PhD Thesis Summary

Scientific supervisor
Prof. Univ.Dr. IOAN ARDELEAN

CLUJ – NAPOCA
2010

CONTENT

INTRODUCTION

Glasses are noncrystaline solid materials that have a disordered structure, but have a local order. The study of materials with vitreous structures gained a special attention due to their manifold applications in domains of science and technology. The oxide glasses unfold a large variety of properties due to the variety of their compounds; these glasses have wide technological applications.

This thesis work is focused on characterizing the structure, the optic and magnetical properties of arsenolite and borate glasses. The study presented in this thesis has as objective the obtaining of new experimental data and the clarification of the physical phenomena which determine the structural behavior of As_2O_3 and B_2O_3 based glasses doped with manganese or iron ions. In order to obtain this information of $xMO\cdot(100-x)[As_2O_3\cdot TeO_2]$, $xMO\cdot(100-x)[As_2O_3\cdot PbO]$ and $xMO\cdot(100-x)[3B_2O_3\cdot Li_2O]$, where MO => MnO or Fe_2O_3 glass systems, with $0 < x < 50\%$ mol MnO or Fe_20_3, they were prepared and investigated by x - ray Diffraction, FT - IR spectroscopy, Raman spectroscopy, electron paramagnetic resonance (EPR) and magnetic susceptibility measurements.

The thesis is structured in four chapters. The first chapter presents, on literature basis, the main results regarding the structure and the properties of As_2O_3 and B_2O_3 based glasses.

Chapter 2 presents theoretical and experimental general aspects regarding the iron and manganese behavior using the IR absorption, Raman spectroscopies, electron paramagnetic resonance and magnetic susceptibility. Chapter 3 describes the experimental techniques used in the studies of glasses. The processing and preparation of the samples are presented. Chapter 4 presents and discusses the experimental results obtained for the investigated glasses. In the end, the general conclusions which emphasize the most important results of this thesis are presented.

CHAPTER 1. THE STUDY OF THE STRUCTURE OF As_2O_3 AND B_2O_3 BASED GLASSES

As_2O_3 and B_2O_3 are the most important glass forming oxides and have been incorporated into various kinds of glass system in order to obtain the desired physical and chemical properties for both scientific and industrial applications. As_2O_3 is a very strong glass formation having a configuration based on pyramidal AsO_3 units, determined by a special dynamics on the As and O bonds, unique properties of the glass systems [1,-3]. The properties of the glasses based the B_2O_3 are due to the fact that the boron atom can assume triangular

and tetrahedral coordination and also to the different ways through which the borate buildings units can be linked together [4-9].

The behavior of various borate species in the glass structure is determined by the nature of modifier oxides (TeO_2, PbO, etc.). In most binary borate glasses the glass properties change almost linearly with composition [10-17]. In binary borate glasses the properties of these show a major deviation from linearity which depends on modifier oxide. The structural reasons for this is generally due to the change in the coordination of boron atom from 3 to 4 and back again. Many technological applications of these glasses depend of this effect since is produces many improvements [18-23].

The introduction of MnO [24-32] or Fe_2O_3 [33-45] into diamagnetic glasses transform them into paramagnetic glasses. The introduction of iron and manganese in small percentages modifies the physical properties of the glasses and the material is more accessible for a complete structural characterization.

In order to extend the available information concerning the interesting class of As_2O_3 and B_2O_3 based glasses we investigated glasses by means of different physical methods. We obtained valuable information concerning the structure and structural changes of the glasses that occur with the addition of transitional oxide metals.

CHAPTER 2. METHODS USED IN THE STUDY OF STRUCTURE AND PROPERTIES OF OXIDE GLASSES

In this chapter some of the methods used in the investigation of the structure and properties of vitreous systems are presented. The study of the structure and properties of oxide glasses with transitional metals ions: IR and Raman spectroscopies, electron paramagnetic resonance and magnetic susceptibility measurements were chosen as investigation methods.

The electromagnetic radiation (EM) with frequencies between 4000 and 400 cm^{-1}, called infrared radiation (IR), is used to obtain information connected to the structure of the compound and as an analytic method to test the purity of the compound. Its application in organic chemistry is known as IR spectroscopy. The radiation is absorbed by organic molecules and converted in molecular vibration energy. When the radiant energy coincides with a specific molecular vibration the absorption appears. The wave length at which the radiation is absorbed by the organic molecule gives information regarding the functional groups presented in the molecule [1-4].

The Raman spectroscopy brings useful contributions to the molecular vibrations study. The interraction mechanism of electromagnetic radiation with the molecular vibration which forms the Raman spectroscopy theoretical basis differs from the one of the process which forms the IR spectroscopy theoretical basis [4].

Another method used in the investigation of the glass system is the electron paramagnetic resonance (RPE). This method is one of the most powerful techniques for local order investigation. RPE is a method widely used to describe the fundamental states and to characterize the vicinities effect on the energetic levels of the paramagnetic centers. The method consists in the study of the electronic split levels of the atoms in the presence of an external magnetic field [6]. The Mn^{2+} EPR spectra are characterized by resonance absorptions at $g_{ef} \approx 4,3$, $g_{ef} \approx 3,3$ and $g_{ef} \approx 2,0$. The resonance line centered at $g_{ef} \approx 4,3$ is corresponding to the isolated Mn^{2+} ions. The line from $g_{ef} \approx 2,0$ is attributed to Mn^{2+} ions involved in magnetic interactions.

The Fe^{3+} EPR spectra are characterized by resonance absorptions at $g \approx 9,7$, $g \approx 6$, $g \approx 4,3$ and $g \approx 2,0$. The resonance line from $g \approx 9,7$ is related to Fe^{3+} ions disposed in rhombic environment. The resonance line at $g \approx 6$ was assigned to an axial distortion of the paramagnetic ions neighborhood. The resonance line at $g \approx 4,3$ is corresponding to the isolated Fe^{3+} ions situated in octahedral, rhombic or tetragonal symmetric distorted neighborhoods. The line from $g_{ef} \approx 2,0$ is attributed to Fe^{3+} ions involved in magnetic interactions.

Along with the EPR spectroscopy, the magnetic susceptibility measurements provide useful information about the valence state and the interaction involving the transitional metal ions in vitreous materials [7-10].

Different vitreous systems with manganese or iron ions were intensively studied by magnetic susceptibility measurements to determine the magnetic behavior and the valence states of these ions in these systems. It was observed that the presence of the manganese or iron ions in different valence states depends on the chemical composition of the vitreous matrix, on the valence of the vitreous network former and modifications and on the preparation of the environment. The magnetic properties of the oxide glasses with manganese or iron ions were assigned to the antiferromagnetic couple between Mn^{2+}-Mn^{2+}, Mn^{2+}-Mn^{3+} and Mn^{3+}-Mn^{3+} [19-26] or Fe -Fe^{3+}, Fe^{2+}-Fe^{2+} and Fe^{3+}-Fe^{2+} ions [11-18].

CHAPTER 3. EXPERIMENTAL TECHNIQUES

We have prepared glasses of the $xMO\cdot(100-x)[As_2O_3\cdot TeO_2]$, $xMO\cdot(100-x)[As_2O_3\cdot PbO]$ şi $xMO\cdot(100-x)[3B_2O_3\cdot Li_2O]$ glass structure, where MO => MnO or Fe_2O_3 with $0 < x < 50$ % mol, used components of reagent grade purity: $MnCO_3$, Fe_2O_3, As_2O_3, H_3BO_3, PbO, Li_2CO_3 şi TeO_2 in suitable proportions to obtain the desired composition. The mixtures were melted in sintered corundum crucibles, introduced in an electric furnace directly at 1250 C and kept for 5 minutes at this temperature. They were quickly cooled at room temperature by pouring onto stainless steel plates**.**

The structure of the samples was analyzed by means of x-ray Diffraction, using powders, with a Bruker D8 Advanced diffract meter.

The FT - IR spectra have been recorded using a Bruker Equinox 55 with a spectral range between 4000 cm^{-1} and 370 cm^{-1}. A MIR, GLOBAR generator cooled with air was used. The detection was carried out with a DLATGS detector with a KBr window. The spectral resolution was about 0.5 cm^{-1}. The samples were prepared using KBr pellet technique.

The Raman spectra were recorded, on bulk samples, at room temperature using an integrated FRA 106/S Raman module attached to Bruker Equinox 55 with a spectral range from 3600 cm^{-1} to 70 cm^{-1}. An Nd.YAG laser with an output power of 500 mW and a 1064 nm radiation was used. The detection was carried out with an ultra sensitive D418-T detector cooled with liquid nitrogen. The spectral resolution was about 1 cm^{-1}.

The EPR spectra were obtained at room temperature with an Adani Portable EPR Spectrometer PS8400 in X-frequency band (9.4 GHz). For these measurements, equal quantities of powders from the investigated samples, closed in glass tubes, were used.

Magnetic susceptibility measurements were performed on a Faraday type balance in the 80 - 300 K temperature range. The sensitivity of the equipment was 10^{-7} emu/g.

CHAPTER 4. RESULTS AND DISCUSSION REGARDING THE STUDY OF $xMO\cdot(100-x)[As_2O_3\cdot TeO_2]$, $xMO\cdot(100-x)[As_2O_3\cdot PbO]$ şi $xMO\cdot(100-x)[3B_2O_3\cdot Li_2O]$ GLASS STRUCTURE, WHERE MO => MnO or Fe_2O_3

In this chapter the results obtained by following the study of the structure and properties of oxide glasses with transitional metals ions by FT- IR and Raman spectroscopies, electron paramagnetic resonance and magnetic susceptibility measurements are presented. The structural changes and magnetic properties with the manganese and iron content were followed.

4.1. Comparative study by FT-IR and Raman spectroscopies of $xMO\cdot(100-x)[As_2O_3\cdot TeO_2]$, $xMO\cdot(100-x)[As_2O_3\cdot PbO]$ şi $xMO\cdot(100-x)[3B_2O_3\cdot Li_2O]$ glasses, where MO => MnO or Fe_2O_3

4.1.1. Comparative study by FT-IR spectroscopy of $As_2O_3\cdot TeO_2$ and $As_2O_3\cdot PbO$ vitreous matrices

In order to obtain new information regarding the role of the modifier in the formation of vitreous matrices, comparative studies by FT-IR spectroscopy were made. The FT-IR spectroscopy is represented in figure 4.1(a,b). The wave length and the structural assignments of FT – IR spectra of $As_2O_3\cdot PbO$ and $As_2O_3\cdot TeO_2$ vitreous matrices are represented in table 4.1.

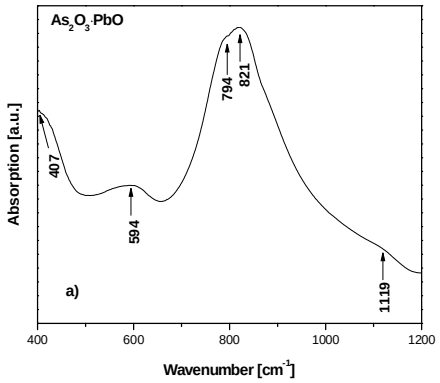

a.

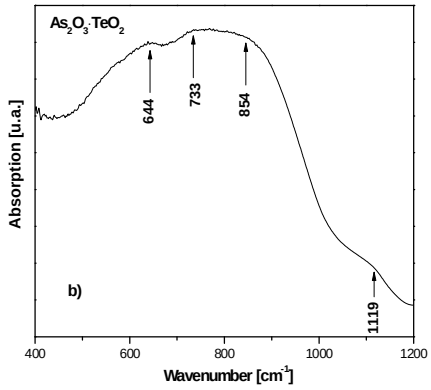

b.

Fig.4.1. FT – IR spectra of vitreous matrices, a. As_2O_3·PbO şi b. As_2O_3·TeO_2.

The FT – IR spectrum of As_2O_3·PbO glass matrix presents five absorption bands at: ~ 1119 cm^{-1}, ~ 821 cm^{-1}, ~ 794 cm^{-1}, ~ 594 cm^{-1} and ~ 407 cm^{-1}(Fig.4.1.a).

The band from ~ 1119 cm^{-1} is due to totally symmetric stretching vibrations of AsO_3 units [5 – 7]. The bands from ~ 821 cm^{-1} and ~ 794 cm^{-1} are due to doubly degenerate stretching vibrations of AsO_3 structural units [5 – 7]. The large band centered at ~ 594 cm^{-1} can be due to totally symmetric bending vibrations of AsO_3 structural units [5-7]. The band from ~ 407 cm^{-1} can be due to vibrations of Pb – O bonds from PbO_4 structural groups [7].

Following As_2O_3·TeO_2 glass matrix spectrum presented in Fig. 4.1.b, four bands can be observed located at: ~ 644 cm^{-1}, ~ 733 cm^{-1}, ~ 854 cm^{-1} and ~ 1119 cm^{-1}. The band from ~ 644 cm^{-1} can be assigned to totally symmetric bending vibrations of AsO_3 units [5-7] and also stretching vibration mode of TeO_4 tbp with bridging oxygen[11]. The band from ~ 733 cm^{-1} can be assigned to the symmetric stretching vibration mode of Te-O bonds in TeO_3 units [15]. The band from ~ 854 cm^{-1} can be assigned to doubly degenerate stretching vibrations of AsO_3 units [5-7] and also to the stretching vibration mode of TeO_3 tp with NBO [11]. The band

from ~ 1119 cm^{-1} can be assigned to totally symmetric stretching vibrations of AsO_3 units [5-7]. These bands, presented in $As_2O_3 \cdot TeO_2$ glass matrix spectrum, confirm the presence of AsO_3, TeO_4 tbp and TeO_3 tp units in the structure of the glass matrix but, due to the broadness of the bands, it can not be told for sure which one of these units is predominant.

Table 4.1.Wavenumber and the structural assignments of FT – IR spectra of $As_2O_3 \cdot PbO$ and $As_2O_3 \cdot TeO_2$ vitreous matrices.

$\tilde{\upsilon}$ [cm^{-1}]		Attribution
$As_2O_3 \cdot PbO$	$As_2O_3 \cdot TeO_2$	
~1119 cm^{-1}	~ 1119 cm^{-1}	Totally symmetric stretching vibrations of AsO_3 units
~ 821cm^{-1}		Doubly degenerate stretching vibrations of AsO_3 structural units
	~ 854 cm^{-1}	Doubly degenerate stretching vibrations of AsO_3 units Stretching vibration mode of TeO_3 tp with NBO
~ 794 cm^{-1}		Doubly degenerate stretching vibrations of AsO_3 structural units
	~ 733 cm^{-1}	Symmetric stretching vibration mode of Te-O bonds in TeO_3 units
~ 594 cm^{-1}	~ 644 cm^{-1}	Totally symmetric bending vibrations of AsO_3 units
~ 407 cm^{-1}		Vibrations of Pb – O bonds from PbO_4 structural groups

4.1.2. Comparative study by FT-IR spectroscopy of $xMO \cdot (100- x)[As_2O_3 \cdot PbO]$ vitreous systems, where MO => MnO or Fe_2O_3

The infrared absorption spectra obtained for $xMO \cdot (1-x)[As_2O_3 \cdot PbO]$ glass system, where MO => MnO or Fe_2O_3, with $0 \leq x \leq 50$ mol%, are presented in figure 4.2-3 and their structural assignments are summarized in table 4.1.

The spectra were discussed on the basis of the method given by Tarte [3] and Condrate [4] by comparing the experimental data of glasses with those of related crystalline compounds. The characteristic absorption bands for crystalline As_2O_3 [5-8], PbO [7,9] and characteristic bands for Fe_2O_3 [18,19] were used as a reference point in the results discussion.

The FT – IR spectra of the investigated glasses suggest a structure formed of AsO_3 and PbO_4 structural units where As_2O_3 plays the role of the glass former and PbO plays the role of the glass modifier. The evolution of the spectra with the addition and the increasing of the MnO content suggest that the manganese ions break up a part of As – O – As, Pb – O – Pb and probably of As – O – Pb bonds. The addition of MnO in the $As_2O_3 \cdot PbO$ glass matrix is leading to a disordering of the glasses structure with the increasing of the MnO content.

The evolution of the absorption bands for FT – IR spectrum of $xFe_2O_3 \cdot (1-x)$ $[As_2O_3 \cdot PbO]$ glasses are determined by the addition of Fe_2O_3 content. . It can be observed to

shift the bands assigned As – O – As vibrations from AsO_3 units due to changing to length As – O – As bonds and interne angles of AsO_3 units, disappears PbO_4 units and appears FeO_6 units The addition of Fe_2O_3 in the As_2O_3·PbO glass matrix determined a disordering of the glasses structure with the increasing of the Fe_2O_3 content.

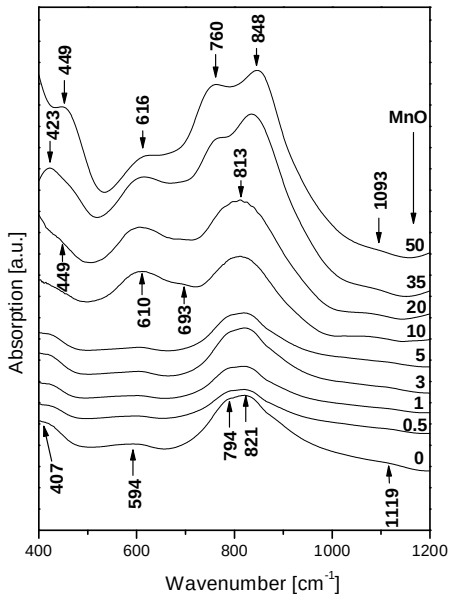

Fig. 4.2. FT – IR spectra of xMnO·(100- x)[As_2O_3·PbO] glasses.

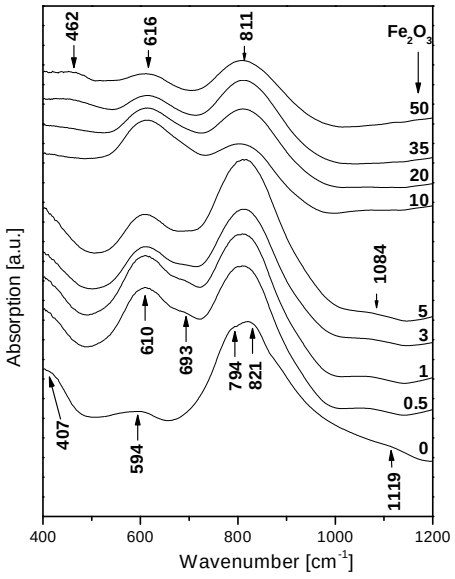

Fig.4.3. FT – IR spectra of xFe_2O_3·(100- x)[As_2O_3·PbO] glasses.

4.1.3. Comparative study by FT-IR spectroscopy of $xMO\cdot(100-x)[As_2O_3\cdot TeO_2]$ vitreous systems, where MO => MnO or Fe_2O

The infrared absorption spectra obtained for $xMO\cdot(1-x)[As_2O_3\cdot TeO_2]$ glass system, where MO => MnO or Fe_2O_3, with $0 \leq x \leq 50$ mol% , are presented in figure 4.4 -5 and their structural assignments are summarized in table 4.1.[16,17]. The characteristic absorption bands for crystalline As_2O_3 [5-8], PbO [7,9], TeO_2 [8,10-15], MnO_2 and Mn_3O_4 [9] and characteristic bands for Fe_2O_3 [18,19] were used as a reference point in the results discussion.

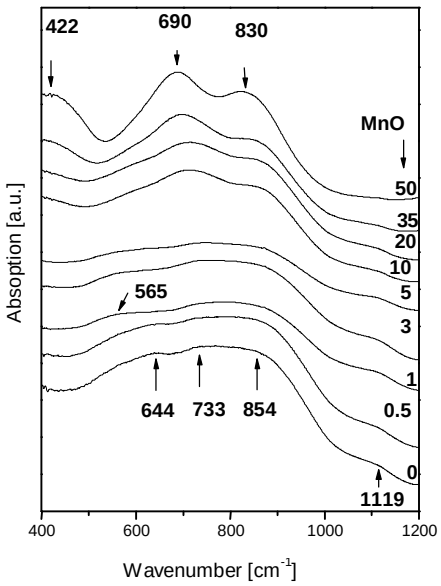

Fig. 4.4. FT – IR spectra of $xMnO\cdot(100- x)[As_2O_3\cdot TeO_2]$ glasses.

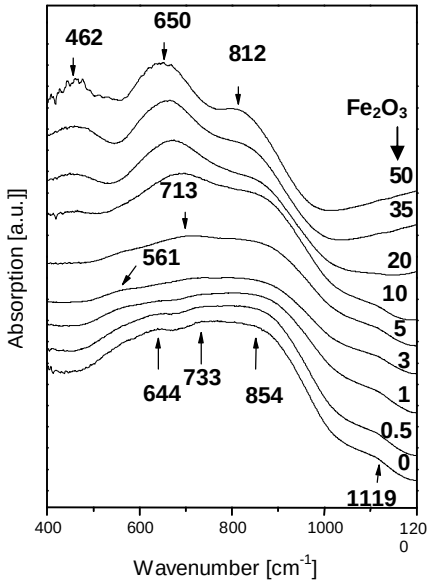

Fig.4.5. FT – IR spectra of $xFe_2O_3\cdot(100- x)[As_2O_3\cdot TeO_2]$ glasses.

This behavior of the studied glasses with the addition and increasing of MnO content suggests that the structure observed in the glass matrix is conserving up to 5 mol% MnO, where the structure takes another form. From a structure dominated by AsO_3, TeO_4 tbp and TeO_3 tp units, the structure became dominated by TeO_4 tbp and MnO_2 units and in a small measure of AsO_3 and TeO_3 tp units. For higher concentrations, it can not be specified exactly which of the last two structural units have the biggest proportion in these glasses. From FT-IR absorption spectra of the investigated glass system it can be observed that the addition and increasing of manganese ions concluded: the contraction of As-O-As bonds from totally symmetric stretching vibrations of AsO_3 units; for $x \geq 10$ % mol there can be an increase in number of As-O-As bonds from AsO_3 units or/and a length these linkage to doubly degenerate stretching vibrations of AsO_3 units and a stretching vibration mode of TeO_3 tp with NBO. It can be remarked from the FT-IR absorption spectra, the gradual transformation of symmetric stretching vibration mode of Te-O bonds from TeO_3 units in TeO_4 (tbp) units and the presence of MnO_2 units. Once, with the addition of iron ions, the $xFe_2O_3 \cdot (100- x)[As_2O_3 \cdot TeO_2]$ glasses behave like $xMnO \cdot (100-x)[As_2O_3 \cdot TeO_2]$ glasses, but in this system the appearance of FeO_6 units can be seen.

4.1.4. Comparative study by FT-IR spectroscopy of $xMnO \cdot (100- x)[As_2O_3 \cdot BO]$ vitreous systems, were BO => TeO_2 or PbO

The infrared absorption spectra obtained for $xMnO \cdot (100- x)[As_2O_3 \cdot BO]$ vitreous systems, where BO => TeO_2 or PbO, with $0 \leq x \leq 50$ mol% MnO, are presented in figure 4.2 and 4.4. Following the infrared absorption spectra, it can be observed that, for $xMnO \cdot (100- x)[As_2O_3 \cdot PbO]$ glass system the most disordered structure to exist for $0 \leq x \leq 5$ mol% MnO and to $xMnO \cdot (100-x)[As_2O_3 \cdot TeO_2]$ glass system for $1 \leq x \leq 5$ mol% MnO. For $x \geq 5$ % mol MnO, manganese ions break up a part of As – O – As, Pb – O – Pb and probably of As – O – Pb bonds, to favor the increase in number of PbO_4 units and appearance of MnO_2 units. For $x \geq 10$ % mol MnO, observed comparatively in both system glasses, the addition of manganese ions suggests for the first system a modification in linkage characteristic units and for the second system an improvement for structural units of $As_2O_3 \cdot TeO_2$ vitreous matrice also linkage characteristic units.

4.1.5. Comparative study by FT-IR spectroscopy of $xFe_2O_3 \cdot (100-x)[As_2O_3 \cdot BO]$ vitreous systems, where BO => TeO_2 or PbO

The infrared absorption spectra obtained for $xFe_2O_3 \cdot (100- x)[As_2O_3 \cdot BO]$ vitreous systems, where BO => TeO_2 or PbO, with $0 \leq x \leq 50$ mol% Fe_2O_3, are presented in figure 4.3 and 4.5.

The evolution of the spectra with the addition and the increasing of the Fe_2O_3 content suggest that the iron ions break up a part of As – O – As, Pb – O – Pb and probably of As – O – Pb bonds. It can be observed a shift in the bands assigned As – O – As vibrations from AsO_3 units due to changing to length As – O – As bonds and interne angles of AsO_3 units, the PbO_4 units disappear and FeO_6 units appear. For $x \geq 5$ % mol Fe_2O_3, observed comparatively in both system glasses, the addition of iron ions suggests for the first system a modification in linkage characteristic units of $As_2O_3 \cdot PbO$ and for the second system an improvement for structural units of $As_2O_3 \cdot TeO_2$ vitreous matrice also linkage characteristic units, appearance of FeO_6 units in both system.

4.1.6. Comparative study by Raman spectroscopy of $As_2O_3 \cdot TeO_2$ and $As_2O_3 \cdot PbO$ vitreous matrices

In order to obtain new information regarding the role of the modifier in the formation of vitreous matrices, there were made comparative studies by Raman spectroscopy. The Raman spectroscopy are presented in figure 4.6(a,b). The wave length and the structural assignments of Raman spectra of $As_2O_3 \cdot PbO$ şi $As_2O_3 \cdot TeO_2$ vitreous matrices are presented in table 4.2.

Table 4.2.Wavenumber and the structural assignements of Raman spectra of $As_2O_3 \cdot PbO$ and $As_2O_3 \cdot TeO_2$ vitreous matrices.

$\tilde{\upsilon}$ [cm^{-1}]		Attribution
$As_2O_3 \cdot PbO$	$As_2O_3 \cdot TeO_2$	
~826 cm^{-1}	~ 816 cm^{-1}	Stretching vibrations of As-O-As
	~ 752 cm^{-1}	Vibrations of the continuous TeO_4 (tbp) network
~ 627 cm^{-1}		Vibrations As – O – As bonds from As_2O units
	~ 580 cm^{-1}	Stretching vibrations of As-O-As
~ 525 cm^{-1}		Vibrations O-As-O bonds from AsO_3 units
	~ 438cm^{-1}	Symmetric bending vibrations of Te – O – Te vertex linkages between different TeO_4 (tbp), TeO_{3+1} polyhedra Stretching vibrations of As-O-As of AsO_3 units
~ 345 cm^{-1}		Bending vibrations of As – O – As from As_2O units

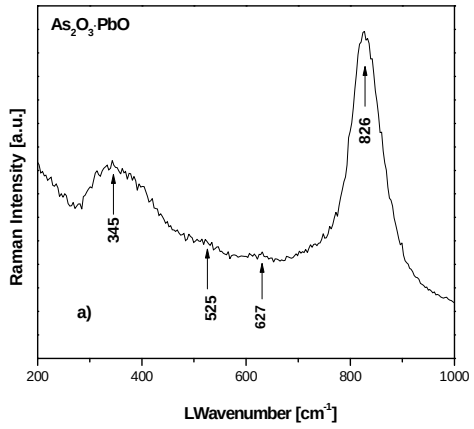

a.

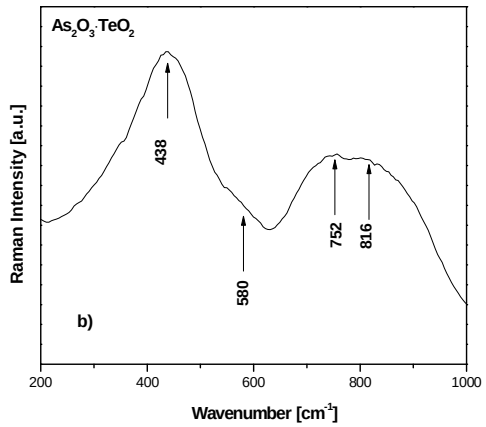

b.

Fig.4.6. Raman spectra of vitreous matrices, a. As_2O_3·PbO şi b. As_2O_3·TeO_2.

The Raman spectrum of As_2O_3·PbO glass matrix presents four bands at: ~ 826 cm^{-1}, ~ 627 cm^{-1}, ~ 525 cm^{-1} and ~ 345 cm^{-1}. The band from ~ 826 cm^{-1} can be assigned to As – O – As stretching vibrations [20]. The band centered at ~ 627 cm^{-1} can be assigned to vibrations As – O – As bonds from As_2O units, the band from ~ 525 cm^{-1} are assigned vibrations O-As-O bonds from AsO_3 units [21]. The band of ~ 345 cm^{-1} are attributed to As – O – As bending vibrations from As_2O units[20,21].

The Raman spectrum of As_2O_3· TeO_2 glass matrix presents four bands at: ~ 816 cm^{-1}, ~ 752 cm^{-1}, ~ 580 cm^{-1} and ~ 438 cm^{-1}. The band from ~ 816 cm^{-1} can be assigned to As – O – As stretching vibrations [20]. The band centered at ~ 752 cm^{-1} can be assigned to vibrations of the continuous TeO_4 (tbp) network [22]. The band of ~ 580 cm^{-1} are attributed to As – O – As stretching vibrations [12]. The band centered at ~ 438 cm^{-1} can be assigned symmetric bending vibrations of Te – O – Te vertex linkages between different TeO_4 (tbp), TeO_{3+1} polyhedra and As – O – As stretching vibrations of AsO_3 units.

4.1.7. Study by Raman spectroscopy of $xMO\cdot(100- x)[As_2O_3\cdot PbO]$ vitreous systems, where MO => MnO or Fe_2O_3

The Raman spectra obtained for $xMO\cdot(100- x)[As_2O_3\cdot PbO]$ vitreous systems, where MO => MnO or Fe_2O_3, with $0 \leq x \leq 50$ mol%, are presented in figure 4.7-8 and their structural assignments are summarized in table 4.2.

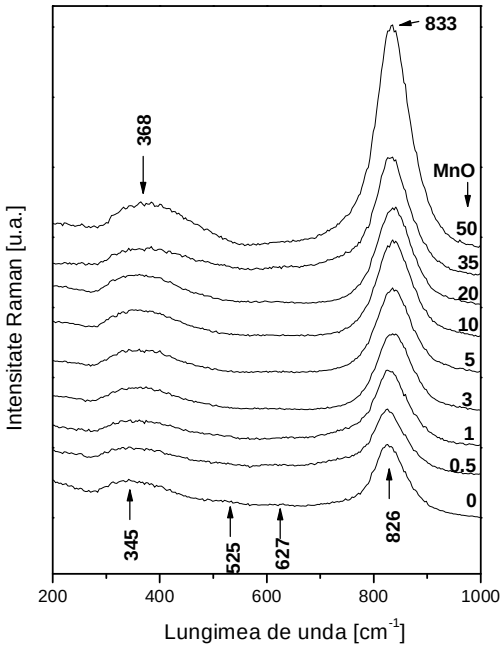

Fig. 4.7. Raman spectra of $xMnO\cdot(100- x)[As_2O_3\cdot PbO]$ glasses.

The addition of MnO in the glass matrix determined an order degree of the vitreous matrix. The intensity of the bands attributed vibrations As – O – As bonds from As_2O units and bending vibrations of As – O – As from As_2O units shift to a higher wave length, that suggests an increase in the As_2O units comparative to AsO_3 units.

To the band from ~ 826 cm^{-1} the addition of manganese ions in the glass matrix determine, for x = 0.5 mol%, an decreasing in intensity, whereupon increasing for higher concentrations. The intensity of bands centered at ~ 627 cm^{-1} and ~ 525 cm^{-1} for x = 0,5 % mol MnO decrease and disappear for x = 1 % mol MnO. The band of ~ 345 cm^{-1} slowly increases with the addition of manganese ions.

To the band from ~ 826 cm^{-1} the addition of iron ions in the glass matrix determines, for x = 0.5 mol%, an increase in intensity, a gradual decrease and disappearance for x = 35 %mol Fe_2O_3 of the bands observed for the glass matrix. For higher concentrations of manganese these bands gradually decrease. The intensity of bands centered at ~ 627 cm^{-1} and ~ 525 cm^{-1} for x = 0,5 % mol Fe_2O_3 increase and shift to ~ 612 cm^{-1} and ~ 501 cm^{-1} whereas

they gradually decrease and disappear for x = 10 % mol Fe_2O_3. The band of ~ 345 cm^{-1} decreases with the addition of iron ions and disappears for x = 20 % mol Fe_2O_3.

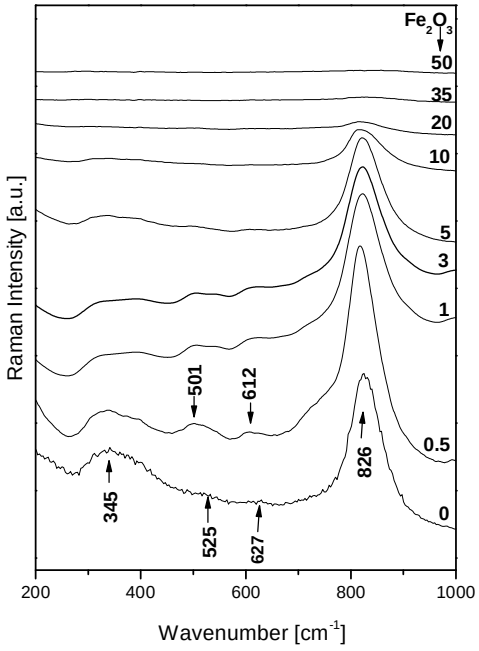

Fig. 4.8. Raman spectra of $xFe_2O_3 \cdot (100- x)[As_2O_3 \cdot PbO]$ glasses.

With the increase of iron ions content in the $As_2O_3 \cdot PbO$ glass matrix, the number of these structural units decreases due to the increasing of the disorder in the studied glasses.

4.1.8. Study by Raman spectroscopy of $xMO \cdot (100-x)[As_2O_3 \cdot TeO_2]$ vitreous systems, were MO => MnO or Fe_2O_3

The Raman spectra obtained for $xMO \cdot (100- x)[As_2O_3 \cdot TeO_2]$ vitreous systems, where MO => MnO or Fe_2O_3, with $0 \leq x \leq 50$ mol%, are presented in figure 4.9-10 and their structural assignments are summarized in table 4.2.

The Raman spectrum of the glass matrix suggests a structure formed from TeO_4 (tbp) and TeO_3 (tp) units where the presence of As – O – As bonds can not be excluded. The addition of manganese ions is leading to a modification of the structure proposed by the spectrum of the glass matrix. Then with the increasing of manganese content the intensity of these bands is increasing, showing that the manganese content favorises the formation of TeO_4 (tbp) and TeO_3 (tp) units.

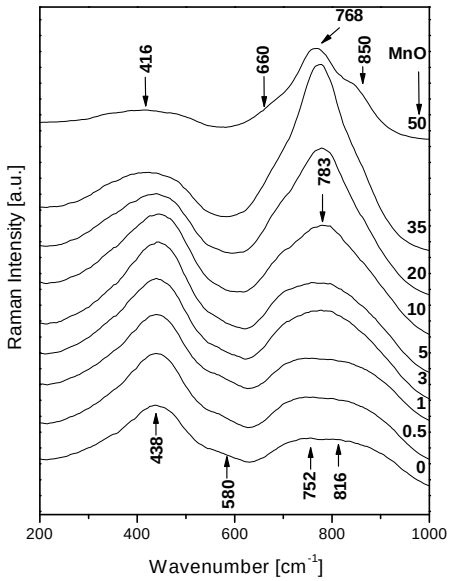

Fig. 4.9. Raman spectra of $xMnO\cdot(100- x)[As_2O_3\cdot TeO_2]$ glasses.

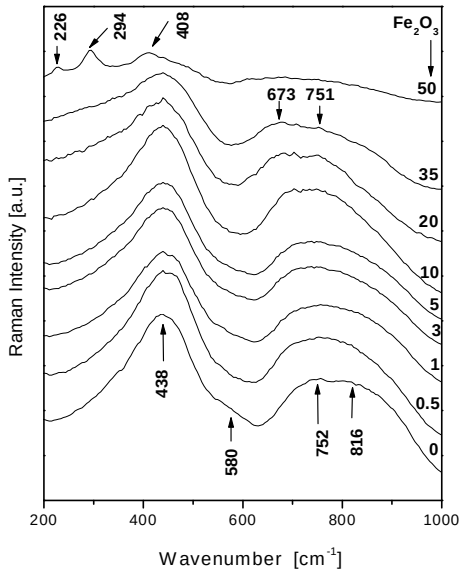

Fig. 4.10. Raman spectra of $xFe_2O_3\cdot(100- x)[As_2O_3\ TeO_2]$ glasses.

The Raman spectra of $xFe_2O_3\cdot(100- x)[As_2O_3\ TeO_2]$ glasses present a significant advance to the TeO_4 (tbp), TeO_{3+1} polyhedra and AsO_3 units represented in Raman spectrum by the ~ 438 cm^{-1} band, comparative with the modifications determined by the addition of manganese ions in vitreous matrix. For high concentrations of iron ions in $xFe_2O_3\cdot(100- x)[As_2O_3\ TeO_2]$ system of glasses, the number of As-O-As linkages appear in Raman spectrum due to stretching vibrations of As-O-As and vibrations of the continuous TeO_4 (tbp) network, show a significant decrease.

4.1.9. Comparative study by Raman spectroscopy of $xMnO\cdot(100- x)[As_2O_3\cdot BO]$ vitreous systems, were BO => TeO_2 or PbO

The addition of MnO to $xMnO\cdot(100- x)[As_2O_3\cdot PbO]$ glass system do not break As – O – As bonds into characteristic units and contribute to their prominence. The addition of manganese ions to $xMnO\cdot(100- x)[As_2O_3\cdot TeO_2]$ glass system for x=50%mol MnO, determined the splitting up of a part of As – O – As, Te-O-Te and the appearance of the TeO_4 (tbp) units against the loss of continuous TeO_4 (tbp) network was observed.

4.1.10. Comparative study by Raman spectroscopy of $xFe_2O_3\cdot(100- x)[As_2O_3\cdot BO]$ vitreous systems, where BO => TeO_2 or PbO

With the increasing of iron ions content in the $As_2O_3\cdot PbO$ glass matrix, the number of these structural units decreased due to the increase of the disorder in the studied glasses (x > 20 % mol) and x = 50 % mol Fe_2O_3 for $xFe_2O_3\cdot(100- x)[As_2O_3\cdot TeO_2]$, when iron ions brought the structural units existing in glass matrices and favoured the appearace of new bands due to bending vibrations of As – O – As.

4.2. Comparative study by FT-IR and Raman spectroscopies of $xMO\cdot(100-x)[3B_2O_3\cdot Li_2O]$ glasses, where MO => MnO or Fe_2O_3

4.2.1. Study by FT-IR spectroscopy of $xMO\cdot(100-x)[3B_2O_3\cdot Li_2O]$ glasses, where MO => MnO or Fe_2O_3

The infrared absorption spectra obtained for $xMO\cdot(1-x)[3B_2O_3\cdot Li_2O]$ glass system, where MO => MnO or Fe_2O_3, with $0 \leq x \leq 50$ mol%, are presented in figure 4.11-13 and their structural assignments are summarized in table 4.3.

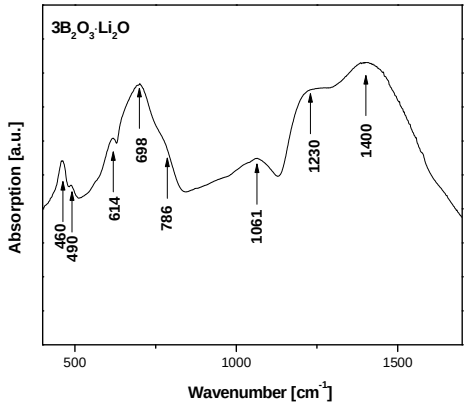

Fig. 4.11. FT – IR spectra of vitreous matrix $3B_2O_3\cdot Li_2O$

Following the infrared absorption spectra obtained for $3B_2O_3 \cdot Li_2O$ vitreous matrix observed on eight bands: : ~ 1400 cm^{-1}, ~ 1230 cm^{-1}, ~ 1061 cm^{-1}, ~ 786 cm^{-1}, ~ 698 cm^{-1}, ~ 614 cm^{-1}, ~ 490 cm^{-1} şi ~ 460 cm^{-1}. The band at ~ 1400 cm^{-1} is assigned to asymmetric stretching vibrations from $B\text{Ø}_3$ şi $B\text{Ø}_2O^-$ groups (Ø represent oxygen atom bridging two boron atoms). The band at ~ 1230 cm^{-1} is attributed to asymmetric stretching vibrations of B – O bonds from triangular ortoborate BO_3^{3-} groups [23-26].

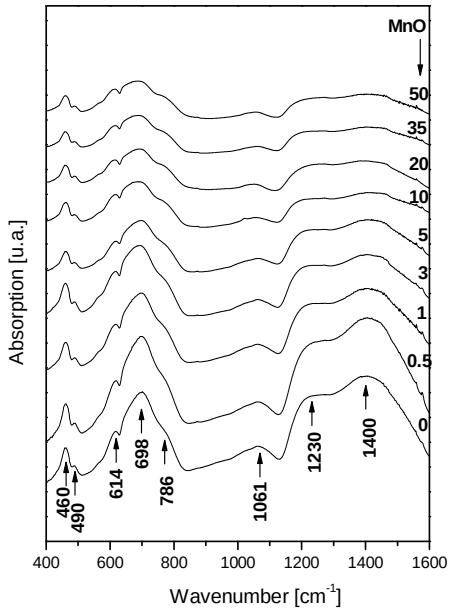

Fig. 4.12. FT – IR spectra of $xMnO \cdot (100-x)[3B_2O_3 \cdot Li_2O]$ glasses

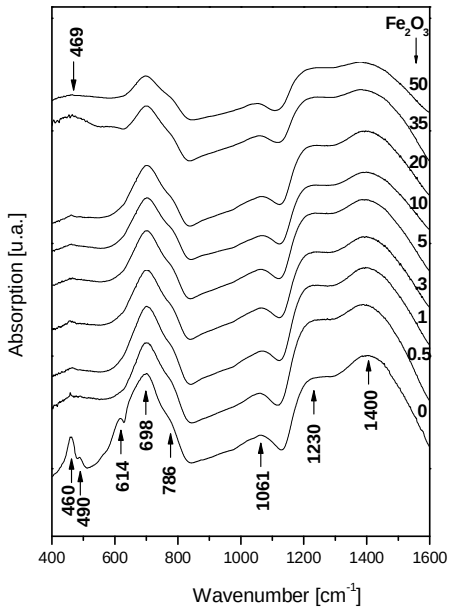

Fig. 4.13. FT – IR spectra of $x\ Fe_2O_3 \cdot (100-x)[3B_2O_3 \cdot Li_2O]$ glasses

Table 4.3.Wavenumber and the structural assignments of FT – IR and Raman spectra of $3B_2O_3 \cdot Li_2O$ vitreous matrix

$\tilde{\upsilon}$ [cm^{-1}]		Attribution	
FT – IR	Raman	FT – IR	Raman
~ 1400 cm^{-1}	~ 1400 cm^{-1}	Asymmetric stretching vibrations from $BØ_3$ şi $BØ_2O^-$ groups	$BØ_2O^-$ triangles linked to other borate triangular units
~ 1230 cm^{-1}		Asymmetric stretching vibrations of B – O bonds from triangular ortoborate BO_3^{3-} groups	
~ 1061 cm^{-1}	~ 1074 cm^{-1}	Stretching vibrations of B – Ø bonds in $BØ_4^-$ tetrahedra from tri-, tetra- and penta-borate groups	Diborate groups
	~ 902 cm^{-1}		Vibrations of orthoborate groups
~ 786 cm^{-1}	~ 791 cm^{-1}	Bending vibrations of $O_3B – O – BO_4$ bonds	Vibrations of rings with six member to one or two BO_4 tetrahedral from tri-, tetra – and penta – borate units
~ 698 cm^{-1}		Bending vibrations of B-O-B bonds from pentaborate groups	
~ 614cm^{-1}		Bending vibrations of O – B – O bonds	
~ 490cm^{-1}	~ 471cm^{-1}	Bending vibrations of B-O-B bonds	Isolated diborate groups
~ 460cm^{-1}		Bending vibrations of O – B – O bonds	

The band at ~ 1061 cm^{-1} is assigned to stretching vibrations of B – Ø bonds in $BØ_4^-$ tetrahedra from tri-, tetra- and penta-borate groups and the band at ~ 786 cm^{-1} is assigned to bending vibrations of $O_3B – O – BO_4$ bonds. The band at ~ 698 cm^{-1} is attributed to Bending vibrations of B-O-B bonds from pentaborate groups. The bands at ~ 614 cm^{-1} and ~ 460 cm^{-1} are assigned to bending vibrations of O – B – O bonds, and the band at ~ 490 cm^{-1} is assigned to bending vibrations of B-O-B bonds.

From FT-IR spectra it can be concluded that the addition of manganese or iron ions in vitreous matrices leads to the increase of the disorder degree.

Also, the structural changes that appeared in $3B_2O_3 \cdot Li_2O$ vitreous matrix with an addition MnO or Fe_2O_3 content, can be studied $Ar=A_4/A_3$ ratio(A_4 - relative number of $BØ_4^-$ tetrahedral borate units, A_3 - relative number of triangular ($BØ_3$ and $BØ_2O^-$) units.

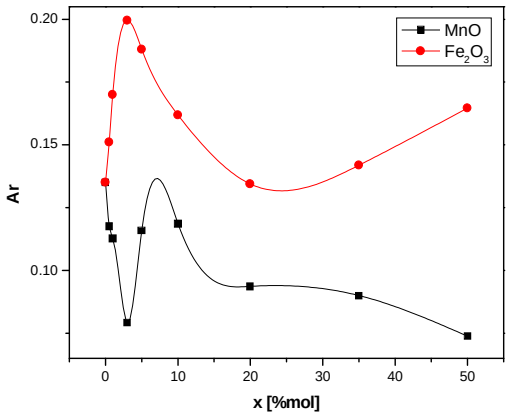

Fig. 4.14. The evolution of Ar ratio with the MnO or Fe_2O_3 content of $xMnO \cdot (100-x)[3B_2O_3 \cdot Li_2O]$ şi $xFe_2O_3 \cdot (100-x)[3B_2O_3 \cdot Li_2O]$

The evolution of the value of this ratio also allows a visualization of the effects determined by the presence of the manganese or iron ions in the matrix. The value Ar<< 1 indicated that BO_3 is dominant related to BO_4.

4.2.2. Study by Raman spectroscopy of $xMO \cdot (100-x)[3B_2O_3 \cdot Li_2O]$ glasses, where MO => MnO or Fe_2O_3

The Raman spectra obtained for $xMO \cdot (1-x)[3B_2O_3 \cdot Li_2O]$ glass system, were MO => MnO or Fe_2O_3, with $0 \leq x \leq 50$ mol%, are presented in figure 4.14-16 and their structural assignments are summarized in table 4.3.

Studying the Raman spectra of $xMO \cdot (1-x)[3B_2O_3 \cdot Li_2O]$ glass system, where MO => MnO or Fe_2O_3, it has been observed that the absorption bands presented in vitreous matrix gradually decreased with an increase in the manganese or iron content, in both glasses system, which suggested an increase of the disorder in these vitreous systems.

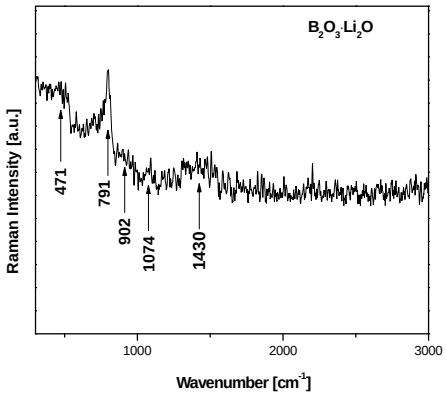

Fig. 4.15. Raman spectra of vitreous matrix $3B_2O_3 \cdot Li_2O$

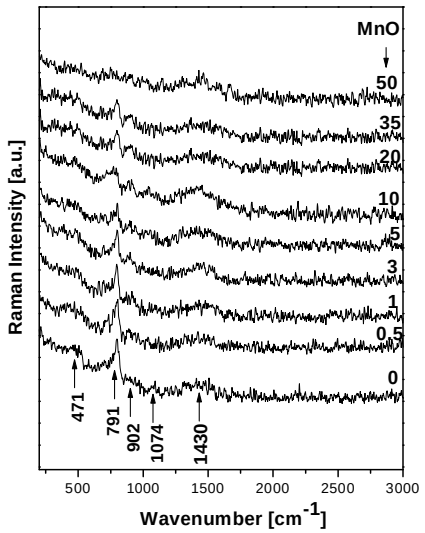

Fig. 4.16. Raman spectra of $xMnO \cdot (100-x)[3B_2O_3 \cdot Li_2O]$ glasses

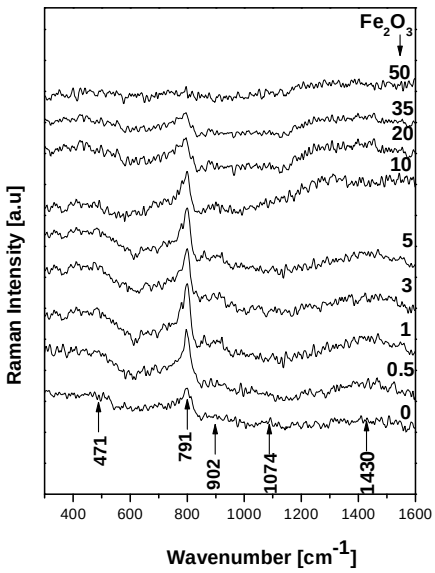

Fig. 4.17. Raman spectra of $x\ Fe_2O_3 \cdot (100-x)[3B_2O_3 \cdot Li_2O]$ glasses

4.3. Comparative study by electron paramagnetic resonance (EPR) and magnetic susceptibility measurements of $xMO\cdot(100-x)[As_2O_3\cdot TeO_2]$, $xMO\cdot(100-x)[As_2O_3\cdot PbO]$ and $xMO\cdot(100-x)[3B_2O_3\cdot Li_2O]$ glasses, where MO => MnO or Fe_2O_3

4.3.1. Comparative study by electron paramagnetic resonance (EPR) of $xMnO\cdot(100-x)[As_2O_3\cdot BO]$, where BO => TeO_2 or PbO and $xMnO\cdot(100-x)[3B_2O_3\cdot Li_2O]$ glasses

In order to obtain more information regarding the behavior of manganese ions in different vitreous matrices [30,31], $xMnO\cdot(100-x)[As_2O_3\cdot BO]$, where BO => TeO_2 or PbO and $xMnO\cdot(100-x)[3B_2O_3\cdot Li_2O]$ glasses were investigated by EPR spectroscopy on a large compositional range, with $0 \leq x \leq 50$ mol%. The EPR spectra of Mn^{2+} for $xMnO\cdot(100-x)[As_2O_3\cdot PbO]$ (S1), $xMnO\cdot(100-x)[As_2O_3\cdot TeO_2]$ (S3) and $xMnO\cdot(100-x)[3B_2O_3\cdot Li_2O]$ (S5) are presented in figure 4.18-20. These spectra present two absorption lines centered at $g_{ef} \approx 4,3$ and $g_{ef} \approx 2,0$ in all systems.

The absorption line centered at $g_{ef} \approx 4,3$ and is due to isolated Mn^{2+} ions [32]. The absorption line centered at $g_{ef} \approx 2,0$ may be attributed to Mn^{2+} species interacting by magnetic coupling[33], dipolar and/ or super exchange, the last ones forming magnetic clusters [32].

The evolution of the spectra is easier to follow considering the dependence of concentration on the EPR parameters, the line - intensity (obtained as an integral of the area under the corresponding EPR signal), J and the line - width, ΔB. The evolution of J and AB reflects the structural transformations which appear in the glass matrices due to the increase of manganese ions content.

The intensity and the line - width of the resonance line from $g_{ef} \approx 4,3$ for all investigated systems is represented in figure 4.21(a,b).

The intensity of the resonance line from $g_{ef} \approx 4,3$ for all investigated glass systems decreases due to the decrease of the isolated manganese ions numbers. The line - width from $g_{ef} \approx 4,3$ for (S1) and (S3) systems decreases due to decrease of Mn^{2+} number and to the structural disorder in glasses with the increase of MnO content. For (S5) glass system the line - width of the resonance line there is an increase in all compositional domains.

The intensity of the resonance line from $g_{ef} \approx 2,0$ can be observed as increasing up to x=14% mol for (S1) system, up to x=8%mol for (S3) system and 20 %mol for (S5) system. The line - width of the resonance line from $g_{ef} \approx 2,0$ for (S1) and (S3) systems increases up to 3 % mol and 5%mol for (S5) due to Mn^{2+} species interacting by magnetic coupling dipole- dipole as the main broadening mechanism. Over this concentration line – the width of the resonance line from $g_{ef} \approx 2,0$ is straight, and it can be assumed that the manganese ions begin to manifest super exchange magnetic interactions.

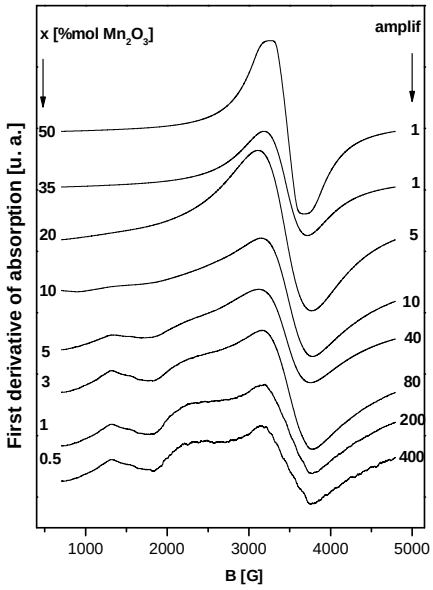

Fig. 4.18. The EPR spectra of Mn^{2+} for $xMnO\cdot(100-x)[As_2O_3\cdot PbO]$ (S1) glass system

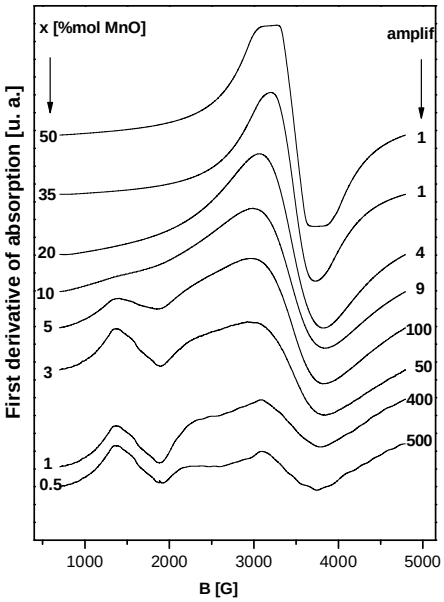

Fig. 4.19. The EPR spectra of Mn^{2+} for $xMnO\cdot(100-x)[As_2O_3\cdot TeO_2]$ (S3) glass system.

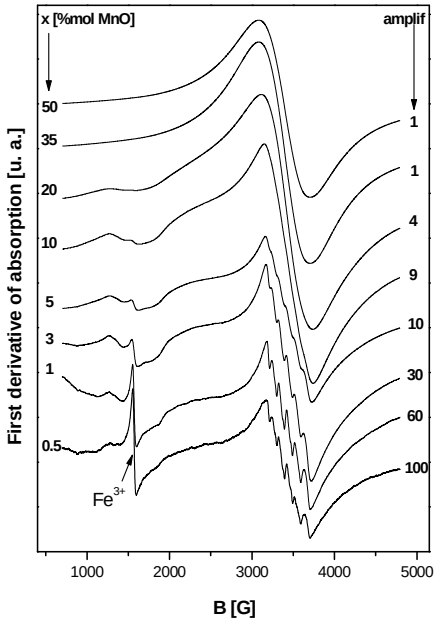

Fig. 4.20. The EPR spectra of Mn^{2+} for xMnO·(100-x)[$3B_2O_3$·Li_2O] (S5) glass system

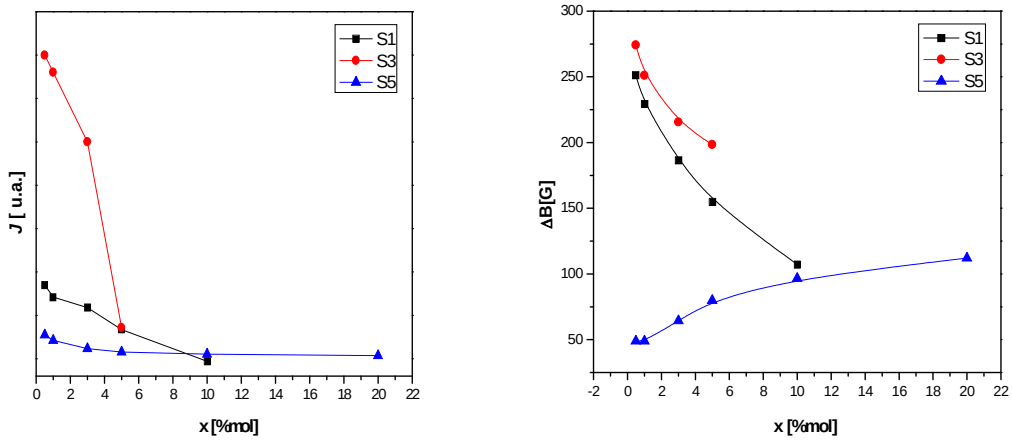

a. **b.**

Fig. 4.21. The dependence on MnO content of the intensity (a) and width(b) of resonance line at $g_{ef} \approx 4,3$ for xMnO·(100-x)[As_2O_3·PbO] (S1), xMnO·(100-x)[As_2O_3·TeO_2] (S3) şi xMnO·(100-x)[$3B_2O_3$·Li_2O] (S5) system glasses

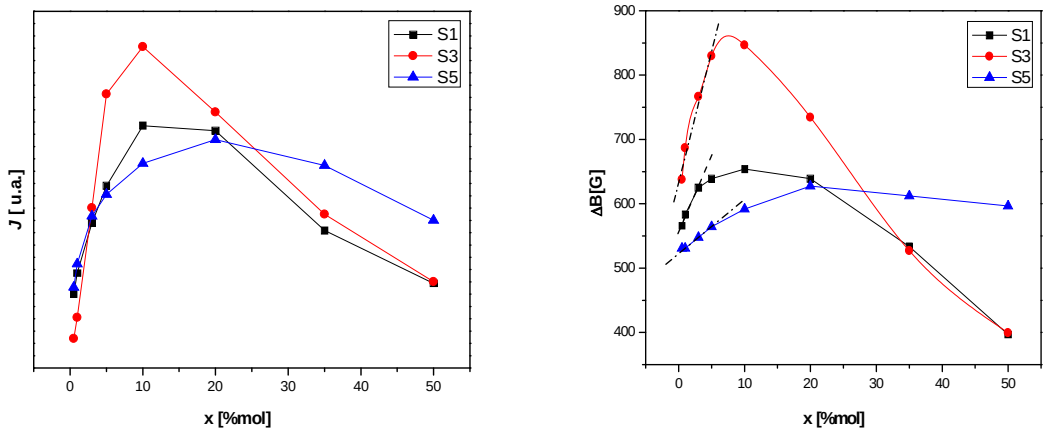

a. **b.**

Fig. 4.22. The dependence on MnO content of the intensity (a) and width b) of resonance line at $g_{ef} \approx 2,0$ for $xMnO\cdot(100-x)[As_2O_3\cdot PbO]$ (S1), $xMnO\cdot(100-x)[As_2O_3\cdot TeO_2]$ (S3) and $xMnO\cdot(100-x)[3B_2O_3\cdot Li_2O]$ (S5) system glasses

Following figure 4.18-20 it can be observed that (S1) and (S3) have had a similar evolution, but (S5) system presented for $0,5 \leq x \leq 5$ %mol (fig.4.20) has a hyperfine sextet[33] at $g_{ef} \approx 2,0$,due to Mn^{2+} isolated ions.

4.3.2. Comparative study by magnetic susceptibility measurements of $xMnO\cdot(100-x)[As_2O_3\cdot BO]$, where BO => TeO_2 or PbO and $xMnO\cdot(100-x)[3B_2O_3\cdot Li_2O]$ glasses

The magnetic susceptibility data are in good agreement with the EPR result. The magnetic behavior of the glasses from $xMnO\cdot(100-x)[As_2O_3\cdot BO]$, where BO => TeO_2 (S3) or PbO (S1) and $xMnO\cdot(100-x)[3B_2O_3\cdot Li_2O]$ (S5) glasses for $3 \leq x \leq 50$ mol% MnO are presented in figure 4.23 - 25.

For (S1) and (S3) system glasses up to $x \leq 3$ %mol and $x \leq 5$ %mol (S5) glass system, the temperature dependence of the reciprocal magnetic susceptibility obeys a Curie law. In this concentration range the manganese ions are predominantly isolated or/and participate in dipole-dipole interractions. At higher concentrations the reciprocal magnetic susceptibility obeys a Curie-Weiss law with negative paramagnetic Curie temperature: (θ_p) characteristic to antiferromagnetic coupled ions by means of super exchange interractions(fig. 4.26). This behavior of manganese ions is confirmed by the shape of the EPR spectra.

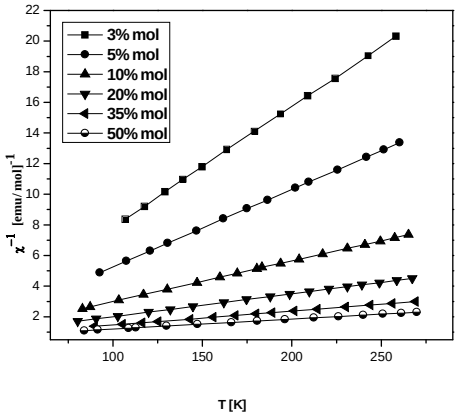

Fig.4.23. The temperature dependence of χ^{-1} for xMnO·(100-x)[As_2O_3·PbO], (S1), $3 \leq x \leq 50$ %mol

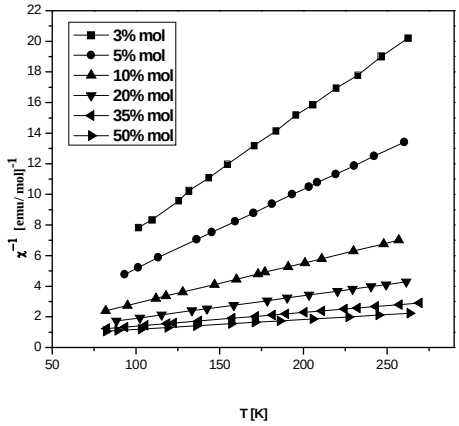

Fig.4.24. The temperature dependence of χ^{-1} for xMnO·(100-x)[As_2O_3·TeO_2], (S1), $3 \leq x \leq 50$ %mol

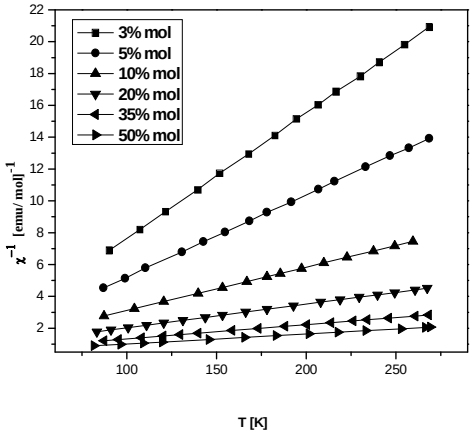

Fig.4.25. The temperature dependence of χ^{-1} for xMnO·(100-x)[$3B_2O_3$·Li_2O] (S5), $3 \leq x \leq 50$ %mol

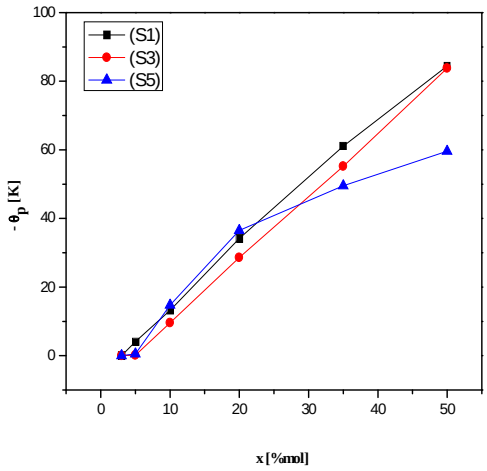

Fig.4.26.Concentration dependence of (θ_p) for sistemele xMnO·(100-x)[As_2O_3·PbO] (S1), xMnO·(100-x)[As_2O_3·TeO_2] (S3) şi xMnO·(100-x)[$3B_2O_3$·Li_2O] (S5).

Using the representation $1/\chi = f(T)$ the molar Curie constants, C_M, the effective magnetic moments and molar fraction of $Mn^{2+}(x_1)$ şi $Mn^{3+}(x_2)$ ions were calculated and represented in tables 4.4 -6.

Tabel 4.4. Molar Curie constants, effective magnetic moments and molar fraction of $Mn^{2+}(x_1)$ şi $Mn^{3+}(x_2)$ ions in xMnO·(100-x)[As_2O_3·PbO] (S1) glasses

x [%mol MnO_2]	$C_M \times 10^2$ [emu/ mol]	μ_{ef} [μ_B]	x_1 [%mol $Mn^{2+}O_2$]	x_2 [%mol $Mn^{3+}O_2$]
3	12,72	5,82	2,68	0,32
5	19,79	5,62	3,43	1,57
10	37,77	5,49	5,55	4,45
20	66,88	5,17	4,92	15,08
35	122,39	5,02	3,77	31,23
50	154,27	4,96	2,68	47,32

Tabel 4.5. Molar Curie constants, effective magnetic moments and molar fraction of $Mn^{2+}(x_1)$ şi $Mn^{3+}(x_2)$ ions in xMnO·(100-x)[As_2O_3·TeO_2] (S3)glasses

x [%mol MnO_2]	$C_M \times 10^2$ [emu/ mol]	μ_{ef} [μ_B]	x_1 [%mol $Mn^{2+}O_2$]	x_2 [%mol $Mn^{3+}O_2$]
3	12,97	5,88	2,87	0,13
5	19,38	5,56	3,12	1,88
10	38,04	5,51	5,75	4,25
20	67,66	5,2	5,49	14,51
35	111,48	5,04	4,41	30,59
50	155,28	4,98	3,58	46,42

Tabel 4.6. Molar Curie constants, effective magnetic moments and molar fraction of $Mn^{2+}(x_1)$ şi $Mn^{3+}(x_2)$ ions in $xMnO\cdot(100-x)[3B_2O_3\cdot Li_2O]$ (S5) glasses.

x [%mol MnO_2]	$C_M\times10^2$ [emu/ mol]	μ_{ef} [μ_B]	x_1 [%mol $Mn^{2+}O_2$]	x_2 [%mol $Mn^{3+}O_2$]
3	12,7	5,81	2,65	0,35
5	19,19	5,54	3,03	1,97
10	36,81	5,42	4,86	5,14
20	72,15	5,19	5,3	14,7
35	112,1	5,06	5,05	29,95
50	158,98	5,01	4,93	45,07

4.3.3. Comparative study by electron paramagnetic resonance (EPR) of $xFe_2O_3\cdot(100-x)[As_2O_3\cdot BO]$, where BO => TeO_2 or PbO and $x\ Fe_2O_3\cdot(100-x)\ [3B_2O_3\cdot Li_2O]$ glasses

In order to obtain more information regarding the behavior of iron ions in $xFe_2O_3\cdot(100-x)[As_2O_3\cdot BO]$, where BO => TeO_2 (S4) or PbO (S2) şi $xFe_2O_3\cdot(100-x)[3B_2O_3\cdot Li_2O]$, glasses were investigated by EPR spectroscopy on a large compositional range, with $0,5 \leq x \leq 35$ mol% Fe_2O_3. The EPR spectra of Fe^{3+} in $xFe_2O_3\cdot(100-x)[As_2O_3\cdot PbO]$ (S2), $xFe_2O_3\cdot(100-x)[As_2O_3\cdot TeO_2]$ (S4) and $xFe_2O_3\cdot(1-x)[3B_2O_3\cdot Li_2O]$ (S6) are presented in figure 4.27-29. These spectra present two absorption lines centered at $g_{ef} \approx 4,3$ and $g_{ef} \approx 2,0$ up to $x \leq 35$%mol Fe_2O_3 systems studied.

The absorption line centered at $g_{ef} \approx 4,3$ is due to isolated Fe^{3+} ions [34-36]. The absorption line centered at $g_{ef} \approx 2,0$ may be attributed to Fe^{3+} species interacting by magnetic coupling, dipolar and/ or super exchange, the last ones forming magnetic clusters [37-41].

The evolution of the spectra is easier to follow considering the dependence of concentration on the EPR parameters, the line - intensity (obtained as an integral of the area under the corresponding EPR signal), J and the line - width, ΔB. The evolution of J and AB reflects the structural transformations which appear in the glass matrices due to the increasing of iron ions content.

The intensity and the line - width of the resonance line from $g_{ef} \approx 4,3$ for all investigated systems is represented in figure 4.30 (a, b). The intensity of the resonance line from $g_{ef} \approx 4,3$ increases for (S2) and (S4) up to 3 % mol and up to 5 % mol for (S6) then decreases for all systems investigated. A line broadening up to 3 % mol from $g_{ef} \approx 4,3$ for these systems can be observed due to increasing of Fe^{3+} isolated number of ions.

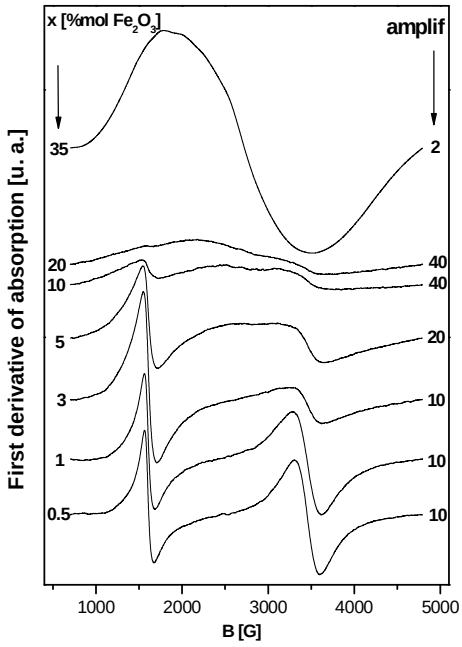

Fig.4.27. The EPR spectra of Fe^{3+} for $xFe_2O_3 \cdot (100-x)[As_2O_3 \cdot PbO]$ (S2) glass system

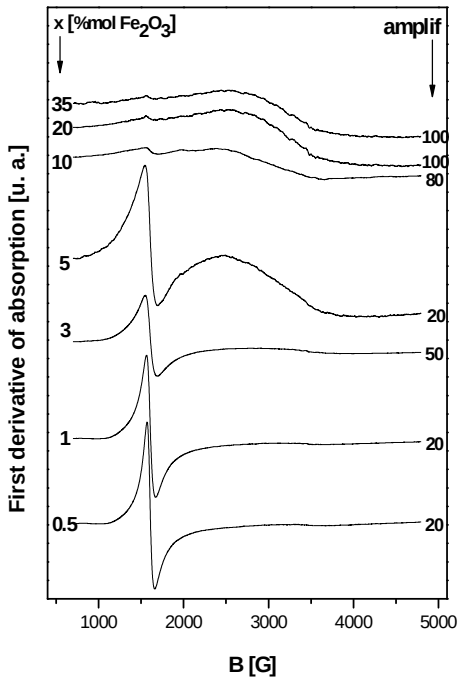

Fig.4.28. The EPR spectra of Fe^{3+} for $xFe_2O_3 \cdot (100-x)[As_2O_3 \cdot TeO_2]$ (S4) glass system

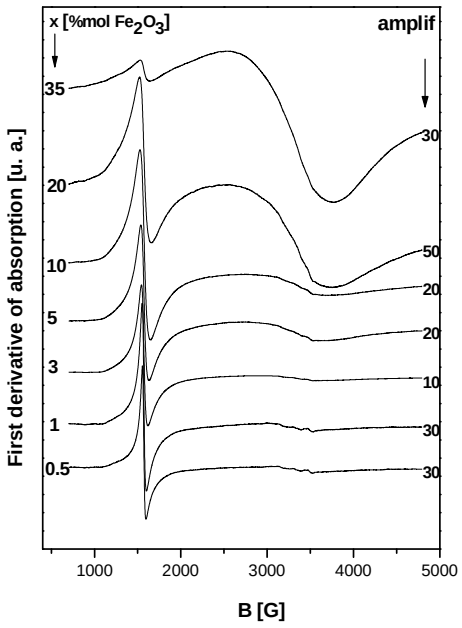

Fig.4.29. The EPR spectra of Fe^{3+} for $xFe_2O_3 \cdot (100-x)[3B_2O_3 \cdot Li_2O]$ (S6) glass system

The intensity and the line - width of the resonance line from $g_{ef} \approx 4,3$ for all investigated systems is represented in figure 4.30 (a, b).The resonance line from $g_{ef} \approx 2,0$ is attributed to Fe^{3+} ions that interact by magnetic coupling, dipolar or/and super exchange interractions can be observed in all compositional domains.

The intensity of the resonance line from $g_{ef} \approx 2,0$ can be observed as increasing up to x=35% mol for (S2) and (S6) system and 10 %mol for (S4) system with increased iron ions content. The line - width of the resonance line from $g_{ef} \approx 2,0$ increased up to 10%mol for (S2) system, and up to 3 % mol for (S4) and 5%mol for (S6) due to Fe^{3+}species interacting by magnetic coupling dipole-dipole. Above this concentration line - width of the resonance line from $g_{ef} \approx 2,0$ can be attributed to dipolar and super exchange magnetic interactions. The $\Delta B = f(x)$ dependence reflects the competion between the broadening mechanism (dipole – dipole interactions, the interactions between ions in diferent valence state and structural disorder) and the narrowing ones (super exchange interactions).

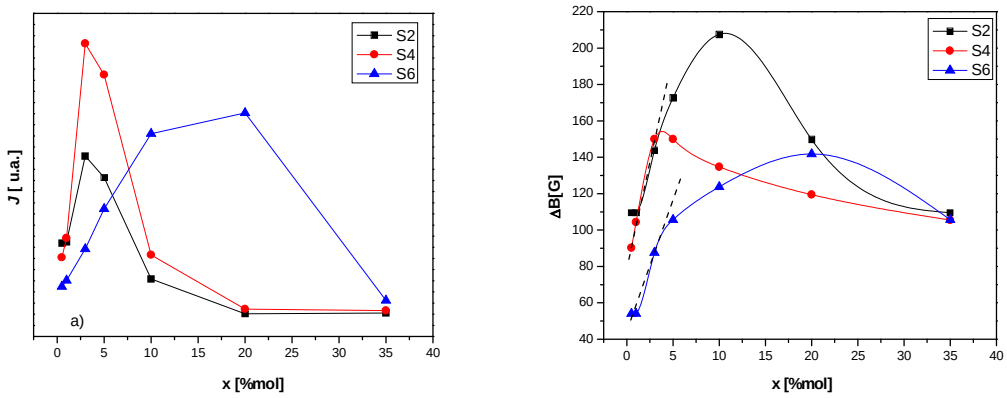

a. b.

Fig. 4.30. The dependence on Fe_2O_3 content of the intensity (a) and width (b) of resonance line at $g_{ef} \approx 4,3$ for $xFe_2O_3 \cdot (100-x)[As_2O_3 \cdot PbO]$ (S2), $xFe_2O_3 \cdot (100-x)[As_2O_3 \cdot TeO_2]$ (S4) and $xFe_2O_3 \cdot (100-x)[3B_2O_3 \cdot Li_2O]$ (S6) glasses

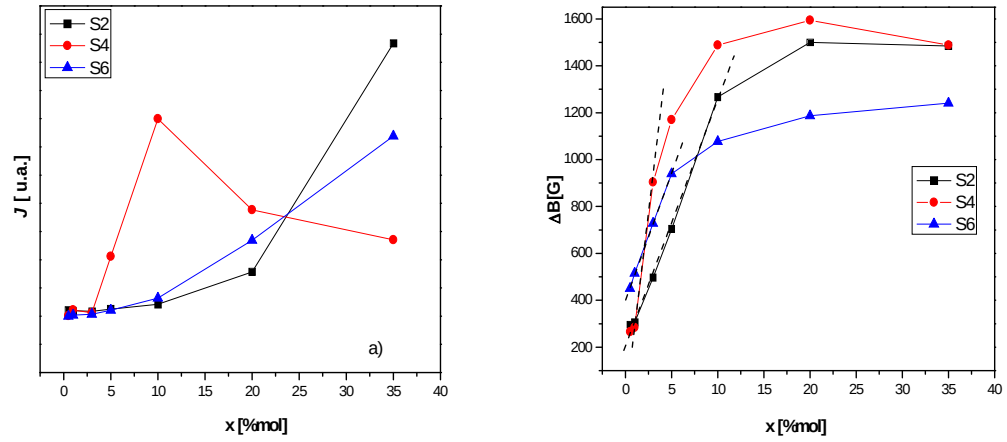

a. b.

Fig. 4.31. The dependence on Fe_2O_3 content of the intensity (a) and width (b) of resonance line at $g_{ef} \approx 2,0$ for $xFe_2O_3 \cdot (100-x)[As_2O_3 \cdot PbO]$ (S2), $xFe_2O_3 \cdot (100-x)[As_2O_3 \cdot TeO_2]$ (S4) and $xFe_2O_3 \cdot (100-x)[3B_2O_3 \cdot Li_2O]$ (S6) glasses

4.3.4. Comparative study by magnetic susceptibility measurements of $xFe_2O_3 \cdot (100-x)[As_2O_3 \cdot BO]$, where BO => TeO_2 or PbO and $xFe_2O_3 \cdot (100-x)\ [3B_2O_3 \cdot Li_2O]$ glasses

The magnetic susceptibility data are in good agreement with the EPR result. The magnetic behavior of the glasses $xFe_2O_3 \cdot (100-x)[As_2O_3 \cdot PbO]$ (S2), $xFe_2O_3 \cdot (100-x)[As_2O_3 \cdot TeO_2]$ (S4) and $xFe_2O_3 \cdot (100-x)[3B_2O_3 \cdot Li_2O]$ (S6) for $3 \leq x \leq 50$ %mol Fe_2O_3 are presented in figure 4.32 - 34.

For (S2) glass systems up to $x \leq 10$ %mol, $x \leq 3$ %mol (S5) glass systems and $x \leq 5$ %mol (S6) glass systems the temperature dependence of the reciprocal magnetic susceptibility obeys a Curie law. In this concentration range the iron ions are predominantly isolated or/and participate in dipole-dipole interactions. At higher concentrations the reciprocal magnetic susceptibility obeys a Curie-Weiss law with negative paramagnetic Curie temperature: (θ_p) characteristic to antiferromagnetic coupled ions by means of super exchange interactions(fig. 4.35). This behavior of iron ions is confirmed by the shape of the EPR spectra.

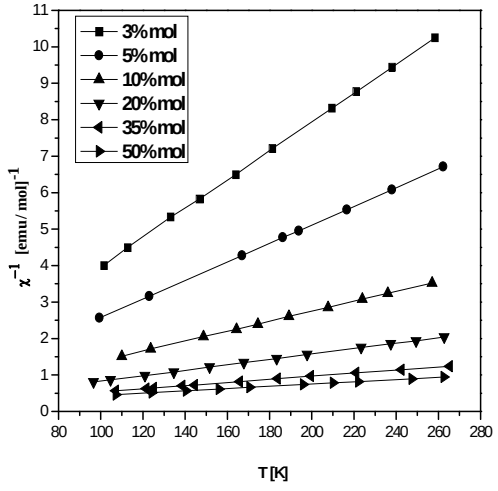

Fig.4.32. The temperature dependence of χ^{-1} for $xFe_2O_3 \cdot (100-x)[As_2O_3 \cdot PbO]$ (S2), $3 \leq x \leq 50$ %mol

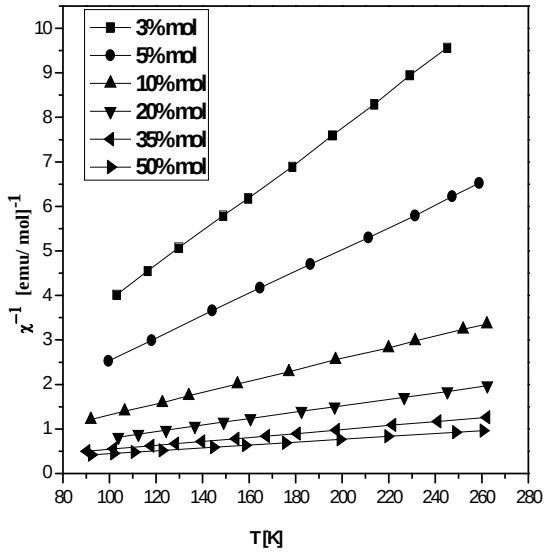

Fig.4.33. The temperature dependence of χ^{-1} for $xFe_2O_3 \cdot (100-x)[As_2O_3 \cdot TeO_2]$ (S4), $3 \leq x \leq 50$ %mol

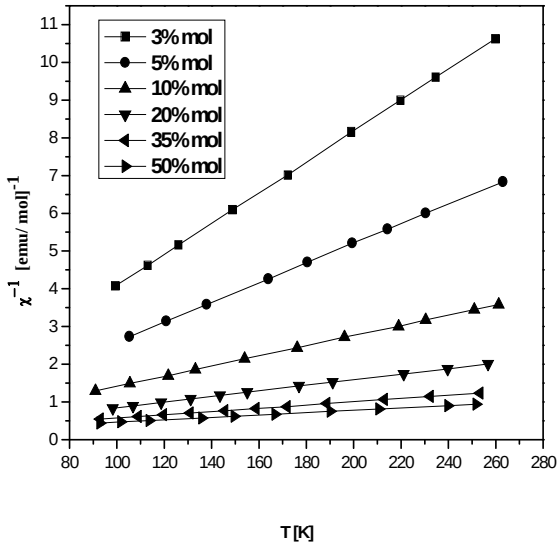

Fig.4.34. The temperature dependence of χ^{-1} for $xFe_2O_3 \cdot (100-x)[3B_2O_3 \cdot Li_2O]$ (S6), $3 \leq x \leq 50$ %mol

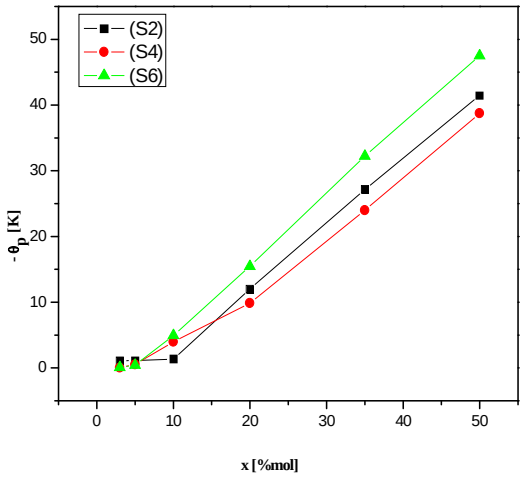

Fig.4.35.Concentration dependence of (θ_p) for sistemele $xFe_2O_3 \cdot (100-x)[As_2O_3 \cdot PbO]$ (S2), $xFe_2O_3 \cdot (100-x)[As_2O_3 \cdot TeO_2]$ (S4) and $xFe_2O_3 \cdot (100-x)[3B_2O_3 \cdot Li_2O]$ (S6), for $3 \leq x \leq 50$ %mol Fe_2O_3

Using the representation $1/\chi = f(T)$ the molar Curie constants, C_M, the effective magnetic moments and molar fraction of $Fe^{3+}(x_1)$ şi $Fe^{2+}(x_2)$ ions were calculated and represented in tables 4.7-9.

Table 4.7. Molar Curie constants, effective magnetic moments and molar fraction of $Fe^{3+}(x_1)$ şi $Fe^{2+}(x_2)$ ions in $xFe_2O_3 \cdot (100-x)[As_2O_3 \cdot PbO]$ glasses (S2)

x [%mol Fe_2O_3]	$C_M \times 10^2$ [emu/ mol]	μ_{ef} [μ_B]	x_1 [%mol $Fe_2^{3+}O_3$]	x_2 [%mol $Fe_2^{2+}O_3$]
3	25,26	5,8	2,61	0,39
5	39,3	5,6	3,32	1,68
10	73,26	5,41	4,76	5,24
20	134,59	5,19	5,3	14,7
35	233,64	5,16	8,29	26,71
50	321,54	5,07	7,67	42,33

Table 4.8. Molar Curie constants, effective magnetic moments and molar fraction of $Fe^{3+}(x_1)$ şi $Fe^{2+}(x_2)$ ions in $xFe_2O_3 \cdot (100-x)[As_2O_3 \cdot TeO_2]$ glasses (S4)

x [%mol Fe_2O_3]	$C_M \times 10^2$ [emu/ mol]	μ_{ef} [μ_B]	x_1 [%mol $Fe_2^{3+}O_3$]	x_2 [%mol $Fe_2^{2+}O_3$]
3	25,71	5,85	2,77	0,23
5	40,16	5,66	3,63	1,37
10	79,11	5,62	6,86	3,14
20	149,92	5,21	6,43	9,29
35	226,76	5,09	6,01	28,99
50	309,59	4,97	3,13	46,87

Table 4.9. Molar Curie constants, effective magnetic moments and molar fraction of $Fe^{3+}(x_1)$ şi $Fe^{2+}(x_2)$ ions in $xFe_2O_3 \cdot (100-x)[3B_2O_3 \cdot Li_2O]$ glasses (S6)

x [%mol Fe_2O_3]	$C_M \times 10^2$ [emu/ mol]	μ_{ef} [μ_B]	x_1 [%mol $Fe_2^{3+}O_3$]	x_2 [%mol $Fe_2^{2+}O_3$]
3	25,42	5,82	2,68	0,32
5	39,43	5,61	3,38	1,62
10	74,23	5,44	5,06	4,94
20	135,68	5,20	5,49	14,51
35	230,94	5,13	7,31	27,69
50	317,46	5,03	5,84	44,16

The results allowed to consider that the magnetic properties of the studied glasses can be explained through magnetic interractions between Fe^{3+} - Fe^{3+} , Fe^{3+}- Fe^{2+} and Fe^{2+}- Fe^{2+} that explain the dependences of RPE parameters concentration.

SELECTED CONCLUSIONS

In this thesis, $xMO \cdot (100-x)[As_2O_3 \cdot TeO_2]$, $xMO \cdot (100-x)$ $[As_2O_3 \cdot PbO]$ and $xMO \cdot (100-x)[3B_2O_3 \cdot Li_2O]$ glasses, where MO => MnO or Fe_2O_3, were comparatively studied in $0 \leq x \leq 50$ %mol . The structural modifications of investigated glass matrices were comparatively followed in function of the manganese or iron ions on the investigated glass matrices were followed.

The study by FT-IR spectroscopy shows that the evolution of the spectra of $xMnO \cdot (100-x)$ $[As_2O_3 \cdot PbO]$ with the addition and the increasing of the MnO content suggest that the manganese ions break up a part of As – O – As, Pb – O – Pb and probably of As – O – Pb bonds. The addition of MnO in the $As_2O_3 \cdot PbO$ glass matrix is leading to a disordering of the glasses structure with the increasing of the MnO content.

The evolution of the absorption bands for FT – IR spectrum of $xFe_2O_3 \cdot (1-x)$ $[As_2O_3 \cdot PbO]$ glasses are determined by the addition of Fe_2O_3 content. . It can be observed to shift the bands assigned As – O – As vibrations from AsO_3 units due to changing to length As – O – As bonds and interne angles of AsO_3 units, disappears PbO_4 units and appears FeO_6 units The addition of Fe_2O_3 in the $As_2O_3 \cdot PbO$ glass matrix determined a disordering of the glasses structure with the increasing of the Fe_2O_3 content.

From FT-IR absorption spectra of the investigated $xMO \cdot (100-x)[As_2O_3 \cdot TeO_2]$ glasses system where MO => MnO or Fe_2O_3, it can be observed that the addition and increasing of manganese ions concluded: the contraction of As-O-As bonds from totally symmetric

stretching vibrations of AsO_3 units; for x ≥10 % mol there can be an increase in number of As-O-As bonds from AsO_3 units or/and a length these linkage to doubly degenerate stretching vibrations of AsO_3 units and a stretching vibration mode of TeO_3 tp with NBO. It can be remarked from the FT-IR absorption spectra, the gradual transformation of symmetric stretching vibration mode of Te-O bonds from TeO_3 units in TeO_4 (tbp) units and the presence of MnO_2 units. Once, with the addition of iron ions, the $xFe_2O_3 \cdot (100- x)[As_2O_3 \cdot TeO_2]$ glasses behave like $xMnO \cdot (100-x)[As_2O_3 \cdot TeO_2]$ glasses, but in this system the appearance of FeO_6 units can be seen.

From FT-IR spectra in $xMO \cdot (100-x)[3B_2O_3 \cdot Li_2O]$ glasses, where MO => MnO or Fe_2O_3 can be concluded that the addition of manganese or iron ions in vitreous matrices leads to the increase of the disorder degree.

The study by Raman spectroscopy shows that the evolution of the spectra the addition of MnO in the $[As_2O_3 \cdot PbO]$glass matrix determined an order degree of the vitreous matrix. The intensity of the bands attributed vibrations As – O – As bonds from As_2O units and bending vibrations of As – O – As from As_2O units shift to a higher wave length, that suggests an increase in the As_2O units comparative to AsO_3 units. With the increase of iron ions content in the $As_2O_3 \cdot PbO$ glass matrix, the number of these structural units decreases due to the increasing of the disorder in the studied glasses.

With the increasing of manganese content in $As_2O_3.TeO_2$ glass matrix, the intensity of these bands is increasing, showing that the manganese content favorites the formation of TeO_4 (tbp) and TeO_3 (tp) units. For high concentrations of iron ions in $xFe_2O_3 \cdot (100-x)[As_2O_3\ TeO_2]$ system of glasses, the number of As-O-As linkages appear in Raman spectrum due to stretching vibrations of As-O-As and vibrations of the continuous TeO_4 (tbp) network, show a significant decrease.

Studying the Raman spectra of $xMO \cdot (1-x)[3B_2O_3 \cdot Li_2O]$ glass system, where MO => MnO or Fe_2O_3, it has been observed that the absorption bands presented in vitreous matrix gradually decreased with an increase in the manganese or iron content, in both glasses system, which suggested an increase of the disorder in these vitreous systems.

The EPR spectra presents the behavior of manganese or iron ions in different vitreous matrices, $xMO \cdot (100-x)[As_2O_3 \cdot BO]$, where MO=>MnO or Fe_2O_3 and BO => TeO_2 or PbO and $xMO \cdot (100-x)\ [3B_2O_3 \cdot Li_2O]$. Glasses were investigated by EPR spectroscopy on a large compositional range, with $0 \leq x \leq 50$ mol%. The absorption line centered at $g_{ef} \approx 4,3$ and is due to isolated Mn^{2+} ions. The absorption line centered at $g_{ef} \approx 2,0$ may be attributed to Mn^{2+} species interacting by magnetic coupling, dipolar and/ or super exchange, the last ones forming magnetic clusters. . The EPR spectra of Fe^{3+} in $xFe_2O_3 \cdot (100-x)[As_2O_3 \cdot PbO]$, $xFe_2O_3 \cdot (100-x)[As_2O_3 \cdot TeO_2]$ and $xFe_2O_3 \cdot (1-x)[3B_2O_3 \cdot Li_2O]$ are presented two absorption lines centered at $g_{ef} \approx 4,3$ and $g_{ef} \approx 2,0$ up to $x \leq 35\%$mol Fe_2O_3 systems studied.

The absorption line centered at $g_{ef} \approx 4,3$ is due to isolated Fe^{3+} ions . The absorption line centered at $g_{ef} \approx 2,0$ may be attributed to Fe^{3+} species interacting by magnetic coupling, dipolar and/ or super exchange, the last ones forming magnetic clusters.

The evolution of the spectra is easier to follow considering the dependence of concentration on the EPR parameters, the line - intensity (obtained as an integral of the area under the corresponding EPR signal), J and the line - width, ΔB. The evolution of J and AB reflects the structural transformations which appear in the glass matrices due to the increase of manganese ions content.

The magnetic susceptibility data are in good agreement with the EPR result. The magnetic behavior of the glasses from $xMnO\cdot(100-x)[As_2O_3\cdot BO]$, where BO => TeO_2 (S3) or PbO (S1) and $xMnO\cdot(100-x)[3B_2O_3\cdot Li_2O]$ (S5) glasses for $3 \leq x \leq 50$ mol% MnO .

For (S1) and (S3) system glasses up to $x \leq 3$ %mol and $x \leq 5$ %mol (S5) glass system, the temperature dependence of the reciprocal magnetic susceptibility obeys a Curie law. In this concentration range the manganese ions are predominantly isolated or/and participate in dipole-dipole interractions. At higher concentrations the reciprocal magnetic susceptibility obeys a Curie-Weiss law with negative paramagnetic Curie temperature: (θ_p) characteristic to antiferromagnetic coupled ions by means of super exchange interractions. This behavior of manganese ions is confirmed by the shape of the EPR spectra. Using the representation $1/\chi = f(T)$ the molar Curie constants, C_M, the effective magnetic moments and molar fraction of $Mn^{2+}(x_1)$ şi $Mn^{3+}(x_2)$ ions were calculated. The magnetic susceptibility data are in good agreement with the EPR result.

The magnetic behavior of the glasses $xFe_2O_3\cdot(100-x)[As_2O_3\cdot PbO]$ (S2), $xFe_2O_3\cdot(100-x)[As_2O_3\cdot TeO_2]$ (S4) and $xFe_2O_3\cdot(100-x)[3B_2O_3\cdot Li_2O]$ (S6) for $3 \leq x \leq 50$ %mol Fe_2O_3 are presented. For (S2) glass systems up to $x \leq 10$ %mol, $x \leq 3$ %mol (S5) glass systems and $x \leq 5$ %mol (S6) glass systems the temperature dependence of the reciprocal magnetic susceptibility obeys a Curie law. In this concentration range the iron ions are predominantly isolated or/and participate in dipole-dipole interactions. At higher concentrations the reciprocal magnetic susceptibility obeys a Curie-Weiss law with negative paramagnetic Curie temperature: (θ_p) characteristic to antiferromagnetic coupled ions by means of super exchange interactions(fig. 4.35). This behavior of iron ions is confirmed by the shape of the EPR spectra. Using the representation $1/\chi = f(T)$ the molar Curie constants, C_M, the effective magnetic moments and molar fraction of $Fe^{3+}(x_1)$ şi $Fe^{2+}(x_2)$ ions were calculated.

REFERENCES

Chapter 1.

[1] I. Ardelean, „Introducere în studiul materialelor oxidice cu structură vitroasă", Ed.NapocaStar, Cluj Napoca, 2002;
[2] G. Srinivasarao, N. Veeraiah,, J. All. Com 327, 52-65(2001);
[3] G. Srinivasarao, N. Veeraiah, J. Phys. Chem. Solids 63,705-717(2002);
[4] D.Becherescu, V.Cristea, F.Marx, I.Menessz, F.Winter, Chimia stării solide, Ed. Şt. şi Encicl., Bucureşti,vol. 1, 1983;
[5] J. Wong, CA.Angell, Glass-Structure by Spectroscopy, Dekker Inc, New York, 1976;
[6] B.E.Warren, H.K.Krutter, O. Morningstat, J. Am. Ceram. Soc, 19, 202 (1936);
[7] L.L.Sperry, J.D. Mackenzie, Phys. Chem. Glasses, 9, 91 (1968);
[8] W.L.Konijnendijk, J.M.Stevels, J. Non-Cryst. Solids, 18, 307 (1975);
[9] F.C.Eversteyn, J.M. Stevels, H.J. Naterman, Phys. Chem. Glasses, 1, 134 (1963);
[10] G. Fuxi, Optical and Spectroscopie Properties of Glass, Springer-Verlag, Shanghai Scientific Technical Pub., Shanghai, 1991;
[11] Y.D.Yiannopoulos, G.D.Chryssikos, E.I.Kamitsos, Phys. Chem. Glasses, 42(3), 164 (2001);
[12] M.G.Ferreira da Silva, B.F.O.Costa, J. Non-Cryst. Solids, 293-295, 534 (2001);
[13] R.Yordanova, Y.Dimitriev, V.Dimitriev, S. Kassabov, D.Klissurski, J.Non-Cryst. Solids, 201, 141 (1996);
[14] W. L. Konijnendijk, J. M. Stevels, J. Non-Cryst. Solids, 18, 307 (1980);
[15] M. Iron, M. Couzi, A.Levasseur, J.Brethous, J.Solid.State Chem., 31, 285, (1980);
[16] T.Furukawa, W.B.White, Phzs.Chem.Glasses 21, 85, (1980);
[17] E. I. Kamitsos, M. A. Karakassides, G.D. Chryssikos, J. Phys. Chem., 90, 4528 (1986);
[18] E. I. Kamitsos, M. A. Karakassides, G.D. Chryssikos, J. Phys. Chem., 91, 1073 (1987);
[19] T.W.Bril, Philips Res. Rep. Suppl., 2, 117 (1976);
[20] E. I. Kamitsos, M. A. Karakassides, G.D. Chryssikos, J. Phys. Chem., 30, 203 (1989);
[21] B.N.Meera, J.Ramakrishna, J. Non-Cryst. Solids, 159, 1 (1993);
[22] K.Witke, T.Hubert, P.Reich, J.Raman.Spectr., 24, 407 (1993);
[23] E. I. Kamitsos, M. A. Karakassides, Phys. Chem. Glasses, 30, 19 (1989);
[24] M.Peteanu, ,,Teză de doctorat" , Universitatea „Babeş-Bolyai", Cluj Napoca, (1989)
[25] P.C.Taylor, P.J.Bray, J.Phys. Chem. Solids, 33, 43 (1972);
[26] I.Ardelean, M.Peteanu, Gh.Ilonca, D.Pop, Solid State Commun., 33, 653 (1980);
[27] A.V. De Wijn, R.E. Van Balderen, J.Kem.Phys. 46, 4 (1967) ;
[28] D.L. Griscom, R.E. Griscom, J. Phys. Chem. Glasses, 12, 19 (1971);
[29] J.W.H. Schreurs, J.Chem. Phys. 69, 2151 (1978);
[30] Al.Nicula, M. Peteanu, I.Ardelean, Studia Univ. Babeş-Bolyai, Physica, 2, 65 (1979),
[31] M. Peteanu, I.Ardelean, S.Filip, I.Todor, G.Salvan, Studia, Univ. Babeş-Bolyai, Physica, XL, 2, 9 (1995);
[32] I.Ardelean, M. Peteanu, S.Filip,V. Simon, I.Todor, Solid State Commun. 105 (5), 339 (1998);
[33] S.K.Mendiratta, E.Guedes de Sousa, J.Mat.Sci. Lett.,7, 733 (1988);
[34] I.Ardelean, M. Peteanu, S.Filip, V. Simon, G.Gyorffy, Solid State Commun., 102 (4), 341 (1997);
[35] I.Ardelean, M. Peteanu, S.Filip, V. Simon, F.Ciorcas, I.Todor, J.Magn.Magn. Mat., 196-197, 257 (1999);
[36] J.Kliava, R.Berger, Y.Servant, J.Emery, J.M.Greneche, J.Trokss, J. Non-Cryst. Solids, 202, 205 (1996);
[37] L.D.Bogomolova, N.A. Krasilnikova, V.L.Bogdanov, V.D.Khaliev, V.V. Mitrofanov, J. Non-Cryst. Solids, 188, 130 (1995);
[38] D.Loveridge, S.Park, Phys.Chem. Glasses, 12, 19 (1971);
[39] I.Ardelean, G. Salvan, M. Peteanu, V. Simon, F.Ciorcas, Mod. Phys.Lett. B, 13 (22-23), 801 (1999);

[40] J.L.Rao, A.Muraly, E.D.Rao, J. Non-Cryst. Solids, 202, 215 (1996);
[41] C.Prakash, S. Husain, R.J. Singh, S.Mollah, J.Alloys Compon., 326, 47 (2001);
[42] E.Guedes de Sousa, S.K.Mendiratta, J.M.Machado Da Silva, Portugal. Phys. 17 (3-4), 203 (1986);
[43] T.Castner, G.S.Newell, W.C.Holton, C.P. Slichter, J.Chem. Phys., 32, 668 (1960);
[44] S.P.Chaudhuri, S.K.Patra, J.Mat.Sci. 35, 4735 (2000);
[45] I.Ardelean, H.H. Qiu, H.Sakata, Matt. Lett., 32, 335 (1997).

Chapter 2.

[1] J. Wong, C. A. Angel, Glass Structure by Spectroscopy, Marcel Dekker inc., New-York, 1976,
[2] I. Ardelean, „Introducere în studiul materialelor oxidice cu structură vitroasă", Ed.Napocastar, Cluj-Napoca, 2002;
[3] N. Avram, G.H. Mateescu, Spectroscopia în infraroşu. Aplicații în chimia organică, Ed. Tehnică, Bucureşti, 1968;
[4] T.Iliescu, Spectroscopie optică moleculară vibrațională şi electronică, Ed. Casa Cărții de Ştiință, Cluj- Napoca, 2000;
[5] S. Aştilean, „Metode şi tehnici moderne de spectroscopie optică", Ed. Casa Cărții de Ştiință, Cluj - Napoca, 2002, p. 5;
[6] I. Ursu, „Rezonanță Electronică de Spin" , Ed. Academiei,Bucureşti, (1965)
[7] C.H.Hurd, Contemp.Phys. 23 (5), 469 (1982);
[8] G..W.Anderson, W.D.Compton, J.Chem.Phys.52, 6166 (1970);
[9] M.S. Seehra, G.Srinivasan, Landolt-Bornstein (New Series), Sub.Volume F3, Springer-Verlag, Berlin, 1994;
[10] G.Toulouse, Contemp.Phys. 2,115 (1977);
[11] N.M.Muray,Magnetic susceptybility, Ed.Interscience, New York, P.1773, 1963;
[12] J.B.Goodenough, Magnetism and Chemical Bond, Ed.Interscience, New York, 1963;
[13] I.Ardelean, G. Salvan, M. Peteanu, V. Simon, F.Ciorcas, Mod. Phys.Lett. B, 13 (22-23), 801 (1999);
[14] I.Ardelean, M.Peteanu, R. Ciceo Lucăcel, „Studii de rezonanță paramagnetică electronică şi magnetice ale unor ioni 3d în sticle pe bază de B_2O_3", Ed. Presa Univesitară Clujeană, 2005;
[15] I.Ardelean, Phys.Stat.Sol. (b) 87K,137 (1978);
[16] I.Ardelean, Solid State Commun. 31, 75 (1979);
[17] E.J.Frieble, L.K.Wilson, A.W.Dozier, D.L.Kinser, Phys.Stat.Sol. (b), 45, 323 (1971)
[18] D.W.Moon, J.M.Aitken, R.K.Mc.Crone, G.S. Ciloszik, Phys.Che. Glasses 16 (5), 91 (1975)
[19] S.Filip, Teză de doctorat, Univ.Babeş-Bolyai, Cluj Napoca, 1996;
[20] C.J.Schinkel, G.W.Rathenou, Physics of Non-Crystaline Solids, North Holland Publ. Co., Amsterdam, 215, 1965;
[21] E.J.Frieble, L.K.Wilson, N.C.Koon, D.L.Kinser, J.Am. Ceram. Soc., 57-237 (1974);
[22] R.J.Landry, J.T. Fournier, C.G.Young, J.Chem.Phys. 46, 1285, (1967);
[23] W.Simpson, Phys.Stat.Solidi, b40, 207, (1970);
[24] R.Hasegawa, Phys.Rev.B b(5) 1631 (1971);
[25] I.Ardelean, Gh.Ilonca, M.Peteanu, Solid State Commun., 52, 145 (1984);
[26] I.Ardelean, Gh.Ilonca, O.Cozar, J. Physique, 49, C8, 1107 (1988).

Chapter 3.

[1] L.F.Bates, Modern Magnetism, p.133, Cambridge University Press. London, 1962;
[2] I.Ardelean, Gh.Ilonca, D.Barbos, Solid State Commun. 40, 769 (1981);
[3] E.Burzo, I.Ursu, D.Ungur, I.Ardelean, J.Mat.Sci. 15, 581 (1980);
[4] E.Burzo, I.Ursu, D.Ungur, I.Ardelean, Mat.Res.Bull. 15, 1273 (1980);
[5] D.L.Griscom, Glass Science and Technology 48, 151 (1990);
[6] P.J.Bray, A.H. Silver, Modern aspects of the vitreous state, vol.1, Butterworth,

London, 1960;
[7] I.Ardelean, Teza de doctorat, Univ.Babeş-Bolyai, Cluj Napoca, 1979;
[8] S.Aştilean, „Metode şi tehnici moderne de spectroscopie optică”, Ed.Casa Cărţii de Ştiinţă, Cluj – Napoca, 2002, p.5;
[9] I.Ardelean, R.Ciceo-Lucăcel, “Fizica şi Tehnologia Materialelor Oxidice. Lucrări Practice”, Ed. Univ. “Babeş-Bolyai”, Cluj-Napoca, 2000;
[10] V.Pop, I.Chicinaş, N.Jumate, ,,Fizica materialelor. Metode experimentale”, Ed.Presa Universitară Clujeană, 2001;
[11] I.Ursu, ,,Rezonanţă electronică de spin”, Ed.Academiei, Bucureşti, 1965.

Chapter 4.

[1] I. Ardelean, **S. Lupşor**, D. Rusu, Solid State Sci. 10, 1384(2008);
[2] I. Ardelean, **S. Lupşor**, D. Rusu, trimis spre publicare la Physica B, decembrie 2009;
[3] P. Tarte, Spectrochim. Acta 18, 467 (1962);
[4] R. A. Condrate, J. Non – Cryst. Solids 84, 26 (1986) ;
[5] G. Srinivasarao, N. Veeraiah, Phys. Stat. Sol. (a) 191, 370(2002);
[6] G. Srinivasarao, N. Veeraiah, J. Phys. Chem. Solids 63, 705(2002);
[7] G. Srinivasarao, N. Veeraiah,, J. All. Com 327, 52 (2001);
[8] D.K. Durga, N. Veeraiah, Bull. Mater. Sci 24 (4), 421 (2001);
[9] F. F. Bentley, L. D. Smithson, A. L. Rozek, Infrared–Spectra and Characteristic Frequencies 700-300 cm^{-1}, Interscience, New York, 1968, p. 103;
[10] O. Noguera, T. Merle-Mejean, A.P. Mirgorodsky, M.B. Smirnov, P. Thomas, J.-C. Champarnaud-Mesjard, J. Non-Cryst. Solids 330, 50 (2003) ;
[11] B.V.R. Chowdari, K.L. Tan, Fang Ling, Solid State Ionics 113 – 115, 711(1998);
[12] C. Jiang, J. Zhang, H. Mao, F. Gan, Glass Technol. 39(6), 200(1998);
[13] M.R. Sahar, K. Sulhadi, M.S. Rohani, J. Mater. Sci. 42, 824(2007);
[14] C. Horea, D. Rusu, I. Ardelean, J. Mater. Sci.: Mater. Electron. 20, 905(2009);
[15] G.E. Rachkovskaya, G.B. Zakharevich, J. Appl. Spectrosc. 74, 86(2007);
[16] I. Ardelean, **S. Lupşor**, D. Rusu, trimis spre publicare la Journal of Materials Science: Materials in Electronics, decembrie 2009;
[17] I. Ardelean, **S. Lupşor**, D. Rusu, trimis spre publicare la Modern Physics Letters B, decembrie 2009;
[18] R. Iordanova, Y. Dimitriev, V. Dimitrov, S. Kassabov, D. Klissurski, J. Non – Cryst. Solids 231, 227 (1998);
[19] R. Iordanova, Y. Dimitriev, S. Kassabov, D. Klissurski, J. Non – Cryst. Solids 204, 141 (1996);
[20] J. O. Jensen, S. J. Gilliam, A. Banerjee, D. Zeroka, S. J. Kirkby, C. N. Merrow, J. Mol. Struct. (Theochem), 664, 145 (2003);
[21] G. N. Papatheodorou, S. A. Solin, Solid State Commun. 16, 5 (1975);
[22] B.V.R. Chowdari, K.L. Tan, Fang Ling, J. Mat. Sci. 35, 2015 (2000);
[23] R. C. Lucacel, C. Marcus, V. Timar, I. Ardelean, Solid State Sci. 9, 850 (2007);
[24] C.P. Varsamis, E.I. Kamitsos, G.D. Chryssikos, Solid State Ionics 136–137, 1031 (2000);
[25] Sherief M. Abo-Naf, Fatma H. El Batal, Moenis A. Azooz, Mat. Chem. Phys. 77, 846 (2002);
[26] S.G. Motke, S.P. Yawale, S.S. Yawale, Bull. Mater. Sci. 25 (10) (2002);
[27] R. Akagi, N. Ohtori, N. Umesaki, J. Non – Cryst. Solids 293, 471(2001);
[28] E. I. Kamitsos, M. A. Karakassides, G. D. Chryssikos, J. Phys. Chem 91(5) 1073 (1987);
[29] H. Ushida, Y. Iwadate, T. Hattori, S. Nishiyama, K. Fukushima, Y. Ikeda, M. Yamaguchi, M. Misawa, T. Fukunaga, T. Nakazawa, S. Jitsukawa, J. Alloys Compd. 377, 167 (2004);
[30] I. Ardelean, F. Ciorcas, M. Peteanu, **S. Lupşor**, G. Salvan, Balkan Phys. Lett. 5 , 860 (1997);

[31] I. Ardelean, M. Peteanu, V. Simon, O. Cozar, F. Ciorcas, **S. Lupşor**, J. Magn. Magn. Mater. 196, 253 (1999);
[32] I.Ardelean, M.Peteanu, Gh.Ilonca, Phys. Stat. Sol. (a) 58, K33(1980);
[33] I.Ardelean, M.Peteanu, R. Ciceo-Lucăcel, "Studii de rezonanță paramagnetică electronică şi magnetice ale unor ioni 3d în sticle pe bază de B_2O_3", Ed. Presa Univ. Clujeană, Cluj Napoca, 2005, p. 171.
[34] J.L.Rao, A.Muraly, E.D.Rao, J. Non-Cryst. Solids, 202, 215 (1996);
[35] R.P.S.Chakradhar, A.Murali, J.L.Rao, Optical Mat., 10, 109 (1998);
[36] I.Ardelean, M.Peteanu, S.Filip, V.Simon, G.Gyorffy, Solid State Commun., 102(4), 341 (1997);
[37] I.Ardelean, M.Peteanu, V.Simon, S.Filip, F.Ciorcaş, I.Todor, J. Magn. Magn. Mat., 196-197, 257 (1999);
[38] I.Ardelean, G.Salvan, M.Peteanu, V.Simon, C.Himcinschi, F.Ciorcas, Mod. Phys. Lett. B, 13(22-23), 801 (1999);
[39] I.Ardelean, H.H.Qiu, H.Sakata, Mat. Lett., 32, 335 (1997);
[40] S.P.Chaudhuri, S.K.Patra, J. Mat. Sci., 35, 4735 (2000);
[41] I. Ardelean, M. Peteanu, V. Simon, G. Salvan, J. Mat. Sci. Technol. 18 (3), 1 (2002).